

An Opportunistic Pathogen Isolated from the Gut of an Obese Human Causes Obesity in Germfree Mice

Na Fei¹, Liping Zhao^{1,2†}

Supplementary Information

Files in this Data Supplement

Supplementary Materials and Methods

Supplementary Results

Supplementary Table 1

Supplementary Table 2

Supplementary Table 3

Supplementary Figure 1

Supplementary Figure 2

Supplementary Figure 3

Supplementary Figure 4

Supplementary Figure 5

Supplementary Figure 6

Supplementary Figure 7

Supplementary Figure 8

Supplementary Figure 9

Supplementary Figure 10

Supplementary Figure 11

Supplementary Figure 12

Supplementary Figure 12

Supplementary Figure 13

Supplementary Figure 14

Supplementary Figure 15

Supplementary Figure 16

Supplementary Figure 17

Supplementary Figure 18

Supplementary Figure 19

Supplementary Figure 20

Supplementary Figure 21

Supplementary Figure 22

Supplementary Figure 23

Supplementary Figure 24

Supplementary Materials and Methods

Human case study.

The volunteer. In August of 2008, a 26-year-old morbidly obese man (weight 174.8 kg, height 172.5 cm, body mass index (BMI) 58.78 kg/m², Taiyuan city, Shanxi Province, China) with coexisting metabolic syndrome came into contact with our lab. During his first visit, the volunteer was administered a general questionnaire, that collected information on demographic characteristics, health status, disease history, gastrointestinal conditions, dietary habit, physical activity, drinking and smoking habits, and etc. The volunteer had no history of surgery in relationship with his morbid obesity, but had several unsuccessful attempts to use pharmaceutical agents for weight loss. The volunteer did not take regular medication and had no family history associated with his symptoms, including obesity, hypertension, hyperlipidemia, hyperinsulinemia, and etc. He had a previous history of pneumonia associated with viral infection when he was 4-month old. On first contact, the volunteer didn't show any symptoms and signs of infection. He consumed one or two drinks of alcohol once or twice per week but did not smoke, rarely took medications and had taken no antibiotics within the previous 3 months. This volunteer provided his informed consent before his admission to the clinical trial. The clinical study was approved by the Ethics Committee of Chinese Clinical Trial Registry (registration number, ChiECRCT-000011).

Dietary intervention and sampling. This volunteer was given a diet composed of whole grains, traditional Chinese medicine and prebiotics (WTP diet) for intervention. He was given 4 cans of gruel per day as staple food contract prepared in the form of cooked

porridge (370 g wet weight per can) then canned by a food manufacturer (Shanghai Meilin Meida Food Co., Ltd.) for 23 weeks. Each can contained 100 g dry ingredients (59 g of carbohydrate, 15 g of protein, 5 g of fat, and 6 g of fiber) providing 336 kcal energy (70 % of carbohydrate, 17 % of protein, 13 % of fat). Fresh fecal samples were collected with 4 or 5 weeks intervals. Whole blood and serum samples were collected with 0, 9 and 23 week (0d, 9w, 23w). All samples were immediately frozen on collection and stored at -80 °C for subsequent analysis.

Anthropometric data, clinical laboratory analysis and biological samples.

Clinical data were collected in Shanxi High-tech Medical Testing Center (China). Body weight and height were determined by electronic column scales (Seca 799/220, Medical Scales and Measuring Systems (Hangzhou) Co. Ltd., China). Blood pressure was measured with a mercury sphygmomanometer in triplicate. Whole blood sample were obtained for blood routine examination by an automated hematology analyzer (Sysmex K4500, Sysmex Corporation, Japan). Serum was collected to characterize biochemical and lipid profiles as well as ultrasensitive C-reactive protein (CRP) on an automatic biochemical analyzer (Sysmex Chemi-180, Sysmex Corporation, Japan). Insulin was detected by an immunoassay system (IMMULITE[®] 1000, Siemens Healthcare Diagnostics Inc., Germany). Serum lipopolysaccharide binding protein (LBP) was determined using an ELISA Kit (USCN Life Science and Technology Co., Ltd, China). Serum adiponectin and interleukin-6 (IL-6) concentrations were also measured using ELISA kits (R&D Systems, Inc., USA, respectively).

Animal Studies.

Animals. Germfree (GF) male C57BL/6J mice were purchased from SLAC Inc. (Shanghai, China), and raised in gnotobiotic isolators with a regular 12-h light cycle (lights on at 0600 h). These GF mice were maintained in Trexler-type flexible-film plastic isolators with sterile food and water until just before death, and surveillance for bacterial contamination was performed by a periodic bacteriologic examination of feces. All mice were first fed with a sterile normal chow diet (NCD, containing 4.62 % fat, 3.45 kcal g⁻¹, from SLAC Inc., Shanghai, China) and water *ad libitum*. When reached 6-10 weeks of age, the animals were divided into 4 groups (n=7) under different treatments for 16 weeks as follows: (1) NCD+LB group: inoculated by gavage with 0.1ml sterile LB medium everyday for one week fed on normal chow diet ; (2) NCD+B29 group: inoculated by gavage with 10¹⁰ cells of B29 per mouse in 0.1ml sterile LB medium everyday for one week under normal chow diet; (3) HFD+LB group: inoculated by gavage with 0.1ml sterile LB medium everyday for one week fed with high-fat diet (HFD, containing 34.9 % fat, 5.21 kcal g⁻¹, D12492, from Research Diets, Inc., New Brunswick, NJ); (4) HFD+B29 group: inoculated by gavage with 10¹⁰ cells of B29 per mouse in 0.1 ml sterile LB medium everyday for one week fed on high-fat diet. Animals in all experimental groups were raised in two cages of 3 or 4 in the gnotobiotic isolators. Each animal's body weight was measured every week with an electronic scale (d=0.01 g) at the same time of day. Energy intake was recorded at the end of the 16 week trial period for 24 hours, 2 mice per cage (Supplementary Figure 13).

In the *Bifidobacterium animalis*-associated germfree mice model, in the first 8weeks, 6- to

10-week-old germfree mice (n=4~6 per group) mice were fed normal chow diet; in the

following 10 weeks, the mice were changed to high-fat diet. HFD+LB group, inoculated by gavage with 0.1ml sterile LB medium once; HFD+B29 group, inoculated by gavage with 10^{10} cells of B29/mouse in 0.1ml sterile LB medium once; HFD+Bifido group, inoculated by gavage with 10^{10} cells of Bifido (*Bifidobacterium animalis*)/mouse in 0.1ml sterile LB medium once (Supplementary Figure 21)..

Conventional (CONV) male C57BL/6J mice were purchased from SLAC Inc. (Shanghai, China). When reached 8 weeks of age, the animals were divided into 4 groups (n=8) under different treatments for 22 weeks which were similar with the GF mice, except that the LB medium or B29 cells was given by gavage everyday during the whole trial period since we have found that B29 couldn't colonize conventional mice gut in our previous study (B29 failed be detected one week after inoculation (data not shown)).

At the termination of the study, blood was collected by retrobulbar intraorbital capillary plexus; all mice were killed by decollation and collected for tissues. White (epididymal, mesenteric, subcutaneous inguina and retroperitoneal) adipose tissues, liver, total gut and muscle were collected, sectioned, and stored in either liquid nitrogen for western blotting or RNeasy (Ambion) for RT-PCR immediately after exsanguination. Heart, lung, liver, spleen, kidney, stomach, intestine and other organs from each mouse were stored in sterile PBS buffer solution pre-added with 0.3g silica gel (0.1mm diameter) for bacterial translocation. All experimental procedures and protocols were approved by the Institutional Animal Care and Use Committee of SLAC Inc..

Modulation of the human gut microbiota analysis by bitter melon in vitro experiment

Fresh stool samples were collected from a health individual (male, 24 years old, live in Shanghai for 3 years) and immediately used for the experiment. After removing visible food particles, the stool samples were diluted into a final concentration of 2% in basic culture medium (Saulnier *et al.*, 2008), and co-cultured with different concentrations of bitter melon powder (0, 3.75, 7.5, 15, and 30 mg ml⁻¹) *in vitro* under anaerobic conditions (10% H₂, 10% CO₂, and 80% N₂). Culture samples were collected at 0, 6, 12, 24, and 48 hours, respectively. Genomic DNA was extracted and subjected to microbial community structure analysis using PCR-DGGE technology according to the methods described below. Bar-coded 454 pyrosequencing technology was also used in this study. Briefly, the extracted genomic DNA was used as template for amplifying the V1 to V3 region of 16S rRNA genes of bacteria. The amplicons from different samples were mixed at an equal ratio for pyrosequencing with the GS FLX platform (Roche, USA). All raw reads were sorted into different samples according to the sample-specific barcode sequences. After removing barcodes and primers, the high-quality sequences were processed using the QIIME package (v1.4.0) for operational taxonomic unit (OTU) delineation using UCLUST at 100% similarity (Caporaso *et al.*, 2010; Edgar, 2010). Representative sequence of each OTU was subjected to RDP classifier (version 2.5) for taxonomical assignment with a bootstrap cutoff of 80% (Dyszynski and Sheldon , 2006). Relative abundances of different phyla, families and genera in each sample were calculated for taxon-based comparisons.

Analysis of gut microbiota by near full-length 16S ribosomal RNA (rRNA) genes clone library.

16S rRNA genes amplification. Fecal DNA of 0d, 9w and 23w of the volunteer was extracted using the InviMag Stool DNA kit (KFml) (Invitek GmbH, Germany), which was used as template to amplify near full-length 16S rRNA genes by universal bacterial primers 27f (5'-AGAGTTTGATCCTGGCTCAG-3') and 1492r

(5'-CGGC/TTACCTTGTACGACTT-3') (Di Cello *et al.*, 1997; Hayashi *et al.*, 2002).

The 25 µl reaction mixture contained 0.75 U of TaKaRa rTaq polymerase (Takara), 1 ×PCR buffer (Mg²⁺ free), 2 mM MgCl₂, 10 pmol of each primer, 200 µM each deoxynucleoside triphosphate (dNTP) and 10 ng of template DNA. A 25 cycles PCR program(Eckburg *et al.*, 2005) was performed with a thermocycler PCR system (PCR Sprint, Thermo electron, Corp., UK). PCR products were purified with DNA Gel Extraction Kit (Genaid) according to the manufacturer's instruction.

Clone library construction and sequencing. The purified amplicons were cloned into pGEM-T Easy vector (LigaFast Rapid DNA ligation system, Promega) according to the manufacturer's instruction, and then transformed into DH5α competent cells (Transgen, Beijing, China). The transformants were selected on Luria-Bertani medium (LB) agar plates containing ampicillin, X-gal and IPTG (TaKaRa Bio Inc.). An average of 300 white clones of each sample was randomly picked for sequencing. The inserts were sequenced bidirectionally using T7 (5'-TAATACGACTCACTATAGGG-3') and SP6 (5'-ATTTAGGTGACACTATAG-3') sequencing primers on ABI 3730xl sequencers (Applied Biosystems). 16S rRNA gene sequences were manually checked and assembled into consensus sequences without vector sequences using Codon Code Aligner (CodonCode Corp.); and sequences containing bases with a quality score of < 20 were

trimmed.

Sequence alignment and phylogenetic analysis of clone library. Clone sequences were checked for potential chimeras using Bellerophon Chimera Check program in the greengenes website (http://greengenes.lbl.gov/cgi-bin/nph-bel3_interface.cgi), and were aligned using the NAST online alignment tool (http://greengenes.lbl.gov/cgi-bin/nph-NAST_align.cgi). These sequences were grouped into operational taxonomic units (OTUs) by DOTUR, at the threshold of 97 % minimum similarity (which is commonly used to define 'species'-level phylotypes) for phylotype binning from an olsen-corrected distance matrix, constructed using ARB (Ludwig *et al.*, 2004) with the furthest neighbor algorithm and 0.001 precision (Schloss and Handelsman 2005). With the most abundant sequence in each OTU being chosen as the representative sequence, the nearest neighbors of these sequences were found by using the RDP query (Dyszynski and Sheldon 2006) which used the RDP II online database. The sequences of the clone library are available at GenBank under accession number JQ940229 - JQ941083.

Denaturing gradient gel electrophoresis (DGGE) analysis of fecal samples.

PCR amplification and DGGE gel analysis. The V3 regions of 16S rRNA genes were amplified by universal bacterial primers P2 (5'- ATTACCGCGGCTGCTGG -3') and P3 (5'-CGCCCGCCGCGCGCGGCGGGCGGGGCGGGGGCACGGGGGGCCTACGGGA GGCAGCAG -3') using the hot-start touchdown protocol described by Muyzer *et al.* (Muyzer *et al.*, 1993) performed with a thermocycler PCR system (PCR Sprint, Thermo

electron, Corp., UK). The 25- μ l reaction mixture contained 1 U of TaKaRa (Takara) rTaq polymerase, 1 \times PCR buffer (Mg^{2+} free), 2 mM $MgCl_2$, 10 pmol of each primer, 200 μ M each deoxynucleoside triphosphate (dNTP) and 10 ng of template DNA. An additional 5 cycles of reconditioning PCR (Thompson *et al.*, 2002) and PCR products purification by polyacrylamide gel electrophoresis (d-PAGE) were performed before DGGE analysis (Zhang *et al.*, 2005) to minimize heteroduplex formation and single-stranded DNA (ssDNA) contamination during PCR amplification. Parallel DGGE analysis was performed using Dcode System apparatus (Bio-Rad). The same amount of the 16S rRNA genes V3 region DNA of each sample were electrophoresed in 8 % (wt/vol) polyacrylamide gels contained a linear 27 % to 50 % denaturant gradient. Electrophoresis was performed in 1 \times Tris-acetate-EDTA buffer at a constant voltage of 200 V and a temperature of 60 $^{\circ}C$ for 240 mins. The DNA bands were stained by SYBR green I (Amresco) and photographed with Gel Image System (Tanon 3500, TanonScience & Technology Co., Ltd., China).

Identification of DGGE bands. DGGE bands were excised from original gels, and eluted in 100 μ l of sterile distilled water at 4 $^{\circ}C$ overnight. A 2 μ l elution was used as template to reamplify the DNA fragments in the excised bands with corresponding primers. PCR products were purified with DNA Gel Extraction Kit (Genaid), ligated with pGEM-T Easy Vector (Promega), and then transformed into DH5 α competent cells (Transgen, Beijing, China). The inserted DNA of positive clones were amplified by corresponding primers and electrophoresed by DGGE to verify the position to the original bands. The clones migrating to the same position with the original bands were sequenced

(Invitrogen). The sequences of excised DGGE bands were submitted to RDP II database to determine their closest isolate relatives with length >1,200 bp. The sequences of excised DGGE bands are available at GenBank under accession number JQ941084 - JQ941137.

Metagenomic sequencing of gut microbiome.

Extraction and purification of DNA from fecal samples. One gram frozen fecal sample aliquot was suspended in sterile ice-cold sodium phosphate buffer (0.1 M SPB: 1 liter contained 1 M Na_2HPO_4 57.7 ml, 1 M NaH_2PO_4 42.3 ml, pH 7.4) by vigorous vortexing. The suspension was centrifuged at 200 g for 5 mins to collect cell pellets. The washed cell pellets were re-suspended in 1ml of buffer Z (10 mM Tris-HCl, 150 mM NaCl, pH 8.0), with 0.3 g of zirconium beads (0.1 mm) and 150 ml of phenol added (pH 8.0). The mixture was then experimentally subjected to two freeze-thaw cycles (10 mins each at $-80\text{ }^{\circ}\text{C}$ and 2 mins at $+60\text{ }^{\circ}\text{C}$); afterwards it was put through two vortexing cycles (5 mins each at 1,700 rpm). The mixtures were placed in the ice for 5 mins after each agitation. The suspension was gently mixed with 110 μl 10 % SDS and ice-bathed for 10 mins; then 150 μl of chloroform-isoamyl alcohol (vol/vol, 24:1) was added and the mixture was centrifuged at 15,000 g for 10 mins. The supernatant was sequentially extracted by equal volumes of phenol, phenol/chloroform-isoamyl alcohol (vol/vol/vol 25:24:1), and chloroform-isoamyl alcohol (vol/vol, 24:1). DNA was precipitated with two volumes of ethanol and 1/10 volume of sodium acetate (3 M, pH 5.2), then collected by centrifugation (15,000 g, 15 mins), air-dried, and dissolved in 100 μl of sterile ddH₂O. RNA was

digested by RNase (1 mg/ml) at 37 °C for 30 mins. The concentration of extracted DNA was determined using a microvolume spectrophotometer (Nanodrop); its integrity and size were checked by 0.8 % agarose gel electrophoresis containing 0.5 mg/ml ethidium bromide. All DNA were air-dried again and stored at -80 °C for subsequent analysis.

Metagenomic sequencing analysis. For samples at 0d, 9w, 23w, paired-end libraries were constructed with different clone insert sizes and subjected to Illumina GA sequencing followed the manufacturer's instruction, which were carried out at Beijing Genomics Institute at Shenzhen. Human sequences were removed by identifying sequences homologous to the Homo sapiens reference genome. Then, high-quality short reads of each DNA sample were assembled using velvet(Zerbino and Birney 2008), Version 1.1.04, a de Bruijn graph-based tool specially designed for assembling very short reads. The parameters for Velvet were k-mer hash length 35, coverage cutoff = 3, minimum contig length = 200, and read category = shortPaired. **Taxonomic assignment.** Gene taxonomic assignments were carried out by classifying the contigs via BLASTP alignment (BLASTP $E < 10^{-5}$, and % identity > 65).against the M5 non-redundant protein database (the integrated NR database).

LPS biosynthetic gene prediction. Thirty KEGG Orthologues (KOs) involved in the LPS biosynthetic pathway were firstly taken from KEGG version 57.0, consisting of 10,778 genes. Metagenomic sequence reads were then searched using BLASTN against the LPS biosynthetic genes library (BLASTN $E < 10^{-10}$, bitscore > 60, and % identity > 70). The number of sequencing reads matching each KO family and was divided by the number of total sequences and multiplied by 100 to calculate a relative abundance. The abundance shifts of LPS biosynthetic genes at the genus level were also calculated.

The raw Illumina read data of all 3 samples has been deposited in the NCBI, under the accession SRA051394.

ERIC-PCR fingerprinting. Enterobacterial repetitive intergenic consensus sequence-PCR (ERIC-PCR) fingerprinting was used to characterize the *Enterobacter cloacae* strain. Bacterial pellets were suspended in 30 µl of Triton X-100 buffer (0.5 % TritonX-100) and let stand for 10 mins at room temperature. The tubes were then centrifuged for 1 mins at 4,000 rpm and the supernatant was used directly for amplification. PCR was performed in a 25-µl reaction containing 80 ng of DNA, 200 mM (each) deoxynucleoside triphosphates, 2.5 U of TaKaRa rTaq polymerase (Takara), 1 × reaction buffer, 2mM MgCl₂, and 0.4 mM of each primer (ERIC 1 (5'-ATGTAAGCTCCTGGGGATTCAC-3') and ERIC 2 (5'-AAGTAAGTGACTGGGGTGAGCG-3')) (Hulton *et al.*, 1991; Versalovic *et al.*, 1991). The amplification conditions were as follows: 7 mins at 95 °C, 30 cycles consisting of 30 s at 95 °C, 1 mins at 52 °C, 8 mins at 65 °C and a final cycle of 16 mins at 65 °C (Versalovic *et al.*, 1991). The PCR products (400 ng) were separated by electrophoresis on a 1% (wt/vol) agarose gel containing ethidium bromide (0.25 mg/ml). ERIC-PCR fingerprints were further analyzed using the UVI band/map software (UVItec, Cambridge, UK).

Sequence-guided bacteria isolation. We cultured this *Enterobacter* population from the volunteer's gut via a "sequence-guided isolation" scheme. The bacteria in a 0.05 g frozen

fecal sample from the volunteer was resuscitated by being suspended in 100 ml sterile LB medium and vibrated for 10 hours at 37 °C. Then the culture was spread plated onto LB agar plates with a serial 10-fold dilution method by using sterile 1 × PBS buffer solution. Afterwards, 300 isolates were selected based on the colony morphology. Then the DGGE analysis were performed to identify these isolates from the LB medium plates as possible *Enterobacter* sp. strains, depending on whether their V3 sequences had migrated to one of the three identical positions of the V3 sequences of the 16S rRNA gene of *Enterobacter* bands in the volunteer's baseline DNA fingerprint (Supplementary Figure 1b). DGGE and ERIC-PCR fingerprinting were performed to classify the selected isolated into different patterns. Representative isolates for each fingerprinting type were identified by 16S ribosomal RNA (rRNA) gene sequencing (performed as described earlier). One predominant isolate (B29) was picked and a spontaneous mutant for rifampicin resistance was selected for animal study.

The near full-length 16S rRNA gene sequence of *Enterobacter cloacae* strain B29 is available at GenBank under accession number JQ940228.

Identification of the *Enterobacter cloacae* B29 strain. Biochemical identification of isolates was performed using the VITEK 2 gram-negative GN card (bioMérieux, Marcy l'Étoile, France). All tests were carried out as specified by the manufacturers' instructions and the results were interpreted by using software version 04.02. We also performed 16S rRNA sequencing, during which the 1.5-kb sequence of 16S rRNA gene was amplified by PCR using universal bacterial primers and sequenced as described earlier, and then its

almost full-length 16S rRNA gene sequence was determined by Sanger sequencing. The nearest neighbors of the B29 16S rDNA sequence was searched against those of the type strains by using RDP SEQMATCH.

Draft Genome Sequence of *Enterobacter cloacae* strain B29

Genome sequencing and draft assembly. The whole genome shotgun sequencing of *Enterobacter cloacae* strain B29 was performed using 454 sequencing with the additional Illumina mate pair data. First, 272,217 reads with a total length of 147,373,094 bp were generated by using Roche 454 GS-FLX System (about 30-fold coverage). This resulted in 55 contigs using the Newbler Assembler (version 2.3, 454 Life Sciences) with the base quality score above 40. Newbler parameters are –consed -a 100 -l 500 –g –m -ml 20. Then, a genomic library with 3 kb inserts was constructed and a total of 3,356,954 paired reads with an average length of 100 bp were obtained using the Illumina HiSeq2000 (about 100-fold coverage), leading to 29 scaffolds with a total length of 4,770,039 bp. The putative protein-coding regions of the 55 contigs were identified by Glimmer 3. The relative-phylogenetic distances between B29 and the other sequenced *Enterobacter* strains were estimated by CVTree2 (K-tuple length = 6), which infers evolutionary relatedness based on oligo-peptide content of complete predicted proteomes using composition vectors.

LPS biosynthetic gene prediction. Scaffolds were searched using BLASTP against a LPS biosynthetic genes library in the LPS biosynthetic pathway derived from the Kyoto Encyclopedia of Genes and Genomes (KEGG, v 57.0) database (BLASTN $E < 10^{-10}$, and % identity > 50). This library consists of 10,778 previously annotated LPS biosynthetic genes derived from 30 KEGG Orthologues (KOs) (Supplementary Figure 4b).

This Whole Genome Shotgun project has been deposited at DDBJ/EMBL/GenBank under the accession AJUQ000000000. The version described in this paper is the first version, AJU010000000.

LPS extraction and detection. Lipopolysaccharide (LPS) extraction from *Enterobacter cloacae* B29 was performed using the LPS extraction kit (iNtRON Biotechnology Co., Seoul, Korea) according to the manufacturer's instruction. Qualitative and quantitative analyses were performed using the chromogenic substrate Limulus amoebocyte lysate (LAL) assay purchased from Associates of Cape Cod Incorporated (ACC, USA). The endotoxin concentrations were calculated from the calibration (0.03125-0.5 Endotoxin Units per ml; EU ml⁻¹) using control standard endotoxin from *E. coli* 0113:H10. *E. coli* 055:B5 LPS (Sigma, L2880; phenol extract) was used as a positive control. Endotoxin activity was expressed as EU per mg LPS (EU mg⁻¹ LPS).

Bacterial culture for quantitative analysis of *Enterobacter cloacae* B29 in mice feces.

During the experiment, every 2 weeks, fecal matter sample was collected for each animal and immediately measured for exact weight, and then spread plated onto LB agar plates with a serial 10-fold dilution method by using sterile 1 × PBS buffer solution. Afterwards the inoculated bacterium B29 was cultured and quantified.

Glucose tolerance test. Mice were fasted for 5-h and baseline blood glucose levels measured with a blood glucose meter (Roche Diagnostics) using blood collected from the

tail vein. Glucose (2 g per kg body weight) was given orally by gavage. Tail vein blood sample was taken at 15, 30, 60, 90 and 120 mins after gavage and immediately measured for blood glucose level.

Serum biochemical analysis in mice. At the end of the experiment, blood sample was collected from each animal by retrobulbar intraorbital capillary plexus. After standing, hemolysis-free serum was generated by centrifugation of blood using depyrogenated tube and preserved at -80 °C for subsequent analysis. Serum insulin was analyzed by an ELISA kit (Merckodia, Uppsala, Sweden). Serum leptin was quantified by an ELISA kit from Millipore Corporation (Billerica, MA). Serum LBP was determined using a Mouse Lipopolysaccharide Binding Protein ELISA Kit (HyCult Biotechnology, Uden, The Netherlands). Serum adiponectin, and SAA concentrations were measured using mouse ELISA kits from R&D Systems (Minneapolis, MN) and Biosource (Invitrogen), respectively. All assays were performed according to the manufacturers' instructions.

Real-time quantitative PCR. Total RNAs from liver, ileum, and epididymal adipose tissue were isolated using an RNeasy Mini Kit (Qiagen) according to the manufacturer's protocol. 2 µg of each total RNA sample was treated with the RNase-free Dnase (Invitrogen). First-strand cDNA was synthesized using random hexamers and Superscript II reverse transcriptase (Invitrogen). PCRs were performed using the Eppendorf Realplex thermocycler. Primer sequences for the targeted mouse genes were as follows:

Tnfa, F: 5'ACGGCATGGATCTCAAAGAC3', R: 5'AGATAGCAAATCGGCTGACG3';

Il1 β , F: 5'TCCATGAGCTTTGTACAAGGA3', R: 5'AGCCCATACTTTAGGAAGACA3';
Il6, F: 5'-GTTCTCTGGGAAATCGTGGA-3', R: 5'-TGTACTCCAGGTAGCTA-3'; *Mcp1*,
 F: 5'TTAAAAACCTGGATCGGAACCAA3', R: 5'GCATTAGCTTCAGATTTACGGGT3';
Tlr4, F: 5'ATGGCATGGCTTACACCACC3', R: 5'GAGGCCAATTTTGTCTCCACA3';
Ikk ϵ , F: 5'ACCACTAACTACCTGTGGCAT3', R: 5'ACTGCGAATAGCTTCACGATG3';
Acc1, F: 5'TAATGGGCTGCTTCTGTGACTC3', R: 5'CTCAATATCGCCATCAGTCTTG3';
Fas, F: 5'GGAGGTGGTGATAGCCGGTAT3', R: 5'TGGGTAATCCATAGAGCCCAG3';
Fiaf, F: 5'CAATGCCAAATTGCTCCAATT3', R: 5'TGGCCGTGGGCTCAGT3'; *Srebp1*, F:
 5'GCATGCCATGGGCAAGTAC3', R: 5'CCACATAGATCTCTGCCAGTGTTG3'; *Ppar γ* ,
 F: 5'TCGCTGATGCACTGCCTATG3', R: 5'GAGAGGTCCACAGAGCTGATT3'; *Zo1*, F:
 5'TTTTTGACAGGGGGAGTGG3', R: 5'TGCTGCAGAGGTCAAAGTTCAAG3';
Occludin, F: 5'ATGTCCGGCCGATGCTCTC3', R:
 5'TTTGGCTGCTCTTGGGTCTGTAT3'. All genes were normalized to housekeeping gene
Gapdh (F: 5'GTGTTCTTACCCCAATGTGT3', R:
 5'ATTGTCATACCAGGAAATGAGCTT3'). Cycle threshold (Ct) values were converted to
 quantification values based on the standard curves. All individual values are expressed as a
 fold change compared to the mean value of the NCD+LB group.

Bacterial translocation. At the end of the experiment, the animals were dissected and
 collected for heart, lung, liver, spleen, kidney, stomach, intestine and other organs. Stored in
 sterile PBS buffer solution pre-added with 0.3 g silica gel (0.1 mm diameter), the samples
 experienced a shock of 1700 rpm for 10 mins. Then 100 μ l supernatant was extracted,

spread plated onto LB agar plates, and counted after being cultured under 37 °C condition for 16 hours.

Statistical analysis. All analyses were performed with the SPSS 17.0 statistical software package (SPSS, Chicago, IL, USA). Data in bar plot are means \pm S.E.M. Normal distribution is tested using Shapiro-Wilk test in SPSS 17.0. If the variable was normally distributed for all the groups, the impact of diet, B29 inoculation, and the interaction between B29 and diet were assessed by two-way ANOVA. Specific group differences were assessed by Student's t-test for comparing differences between two groups or one-way ANOVA followed by post hoc (Turkey's multiple comparison test) for comparing differences between multiple groups. If the variable was not normally distributed for all the groups, the Kruskal–Wallis H-test were performed to assess the diet and B29 effect, followed by the Mann–Whitney U test to identify specific group differences when the Kruskal–Wallis test showed significance ($P < 0.05$). Different letters in tables denoted significant difference ($P < 0.05$); the same letters denotes no significant difference existed ($P > 0.05$). * or ** represent data significantly different at $P < 0.05$ or $P < 0.01$ level.

Supplementary results

Bitter melon markedly modulated the human gut microbiota in *in vitro* experiment

Principal component analysis (PCA) based on the PCR-DGGE fingerprinting data showed that, although incubation time explained the largest proportion of total variance of gut microbiota community structure (33.8%), treatment of bitter melon also induced marked alterations along the second (24.3%) and third (10.8%) principal components (Supplementary Figure 1a and b). Band 20 and band 36 showed the most significantly altered variables as identified with PCA (Supplementary Figure 1a). By sequence analysis, these two bands are identified to be related to *Faecalibacterium prausnitzii* ATCC 27768 (100%) and *Desulfovibrio intestinalis* strain KMS2 (92%), respectively. Bar-coded 454 pyrosequencing also showed that bitter melon markedly inhibited the growth of the phylum *Proteobacteria*, particularly *Desulfovibrionaceae* and *Enterobacteriaceae*, and enriched the *Faecalibacterium*, one of most abundant genera in the phylum *Firmicutes* (Supplementary Figure 1c).

Changes of endotoxin load, inflammatory tone and improvement of metabolic health phenotypes of the morbidly obese volunteer during weight loss.

On presentation, along with being the morbidly obese, the volunteer also suffered from series of comorbidities, including diabetes (fasting plasma glucose 8.95 mmol/L, fasting plasma insulin 58.7 μ IU/ml, glycated haemoglobin (HbA1c) 7.58 % and HOMA insulin resistance (HOMA-IR) 23.35), hypertension (systolic blood pressure 150 mmHg; diastolic blood pressure 110 mmHg), and hyperlipidemia (triglycerides 2.68 mmol/L, total cholesterol 5.53 mmol/L). Impaired liver function (aspartate aminotransferase 122 U/L, alanine

aminotransferase 97 U/L, gamma-glutamyl transferase 168 U/L) were also identified.

This volunteer was given a diet composed of whole grains, traditional Chinese medicine and prebiotics (WTP diet). During the 23-week dietary intervention, changes of endotoxin load, inflammatory tone and improvement of metabolic health phenotypes of the morbidly obese volunteer were shown in Table 1. Compared to the baseline (0d) value, the volunteer achieved marked weight loss after completing the dietary intervention. After 9 weeks, the volunteer's body weight reduced to 144.8kg, a 17.2 % (30.1 kg) less than the initial value. Finally at 23w, the amount weight lost reached 51.4 kg (29.4 % of initial body weight), with his BMI decreasing from 58.78 kg/m² at baseline to 48.66 kg/m² at 9w and 41.50 kg/m² at 23w. At the same time, the volunteer also experienced complete resolution or obvious improvement in diabetes, hyperlipidemia, and hypertension. At 9w, the glucose homeostasis parameters showed a complete resolution of diabetes by the dietary intervention (fasting plasma glucose 4.76 mmol/L, fasting plasma insulin 25.8 μIU/ml, HbA1c 5.44 % and HOMA insulin resistance (HOMA-IR) 5.46). Hypertension also experienced complete resolution with systolic blood pressure and diastolic blood pressure decreased to 120 mmHg and 80 mmHg, respectively. Hyperlipidemia improved with triglycerides and total cholesterol decreased to 1.72 mmol/L and 4.64 mmol/L. The concentrations of liver function markers in blood—aspartate aminotransferase, alanine aminotransferase and the γ-glutamyl transpeptidase—reducing to 51 U/L, 50 U/L and 49 U/L respectively, revealed obvious improvement of the impaired liver function. The anthropometric indices and biochemical measurements at 23w showed the diet having an essential effect on maintaining healthy systemic metabolic homeostasis. At 23w, the continuous measures demonstrated that blood

glucose levels and blood pressure stayed within the normal range (fasting plasma glucose 5.40 mmol/L, fasting plasma insulin 23.0 mmol/L, HbA1c 4.52 % and HOMA insulin resistance (HOMA-IR) 5.52, systolic blood pressure 120 mmHg and diastolic blood pressure 75 mmHg). The hyperlipidemia and impaired liver function were also resolved after the diet intervention (triglycerides 1.18 mmol/L and total cholesterol 4.78 mmol/L, aspartate aminotransferase 31 U/L, alanine aminotransferase 33 U/L, γ -glutamyl transferase, 59 U/L). The endotoxin load and inflammatory tone of the volunteer were also alleviated as demonstrated by the decreasing inflammatory indicators (LBP, C-reactive protein (CRP), interleukin 6 (IL-6) and adiponectin). The plasma CRP concentration reduced from 14.1 mg/L to 9.4 mg/L at 9w, and 9.51 mg/L at 23w. IL-6, a pro-inflammation cytokines, was also much lower than the initial value, (from 6.71 pg/ml to 4.46 pg/ml at 9w and 2.76 pg/ml at 23w). Adiponectin, an anti-inflammation factor, increased after the dietary intervention (from 2.00 μ g /ml to 2.09 μ g /ml at 9w and 4.27 μ g /ml at 23w). The plasma LBP (an important carrier of blood LPS) level decreased from 7.03 μ g/ml to 2.29 μ g/ml at 9w, and rebounded at 23w (4.78 μ g/ml) but still remained much lower than the baseline, indicating that the dietary intervention changed the antigen load from the gut bacteria in the blood.

Changes of endotoxin-producing *Enterobacter* in the morbidly obese volunteer during weight loss.

Phylogenetic analysis of 16S rRNA gene clone library. We used the near full-length 16S ribosomal RNA gene sequence libraries of the fecal microbiota to profile the microbial composition of the morbidly obese volunteer's gut microbiome. Sequences for 3 time points

were 299, 291 and 297, respectively. A total of 855 nonchimeric near full-length 16S rRNA gene sequences were subjected to phylogenetic analysis. The diversity of fecal bacteria community of each library and the combined library were calculated by Good's coverage which was > 90 %, indicating that the 16S rRNA gene sequences from these samples represented the majority of the human intestinal bacteria community in this study (data not shown). Based on 97 % sequence similarity, the total clones were assigned to 78 OTUs. The three dominant phyla were *Firmicutes*, *Proteobacteria* and *Bacteroidetes*, which together constituted nearly 100 % of the reads (17.31 %, 46.29 %, 36.40 %, respectively). The detailed distribution of the relative abundance of the genera in each sample was shown in Supplementary Figure 2. *Enterobacter* spp. (subdivision of the phylum *Proteobacteria*, class *Gamma-proteobacteria*, family *Enterobacteriaceae*), usually at a low frequencies in the adult gut, changed from 34.98 % at 0 day to 1.77 % at 9 week, and 0 % at 23 week (Supplementary Figure 2).

Structural changes of gut microbiota and identification of *Enterobacter* spp. in the DGGE fingerprint based on the V3 region of the 16S rRNA gene. The dominant gut bacterial community structure from the volunteer at six sampling times was illustrated in 16S rRNA gene V3 region (Supplementary Figure 3a). Most of V3 DGGE bands were identified by sequencing; these are listed in Supplementary Figure 3b. The identification of V3 DGGE bands provided the phylogenetic information at species level for each band. The three dominant V3 DGGE bands (b3, b4 and b5) in the volunteer's baseline DNA fingerprint were identified to contain V3 sequences of the 16S rRNA gene of *Enterobacter* spp. Other

dominant V3 DGGE bands were identified as members of phylum *Firmicutes* and *Bacteroidetes* (Supplementary Figure 3b).

Metagenomic sequencing analysis of gut microbiota structure. An average of 6 Gb (5.8 Gb at 0d, 6.1 Gb at 9w and 6.1 Gb at 23w, respectively) of sequence was generated for each sample, allowing us to capture most of the novelty. We first assembled the short Illumina reads into longer contigs using velvet (each sample independently), which could then be analysed and annotated by standard methods. The Illumina GA reads was assembled into a total of 0.18 million contigs of a length > 166 bp, giving a total contig length of 0.35 Gb, with an N50 length of 6.3 kb and N90 length of 670 bp.

To investigate the phylogenetic composition of the 3 samples from this volunteer, we mapped metagenomic contigs to reference genomes. The vast majority of sequences (99.2 %) in the newly sequenced 3 samples belong to bacteria—only 0.3 % of the reads could be classified as eukaryotes and 0.2 % as archaea, all others together only comprised 0.3 %. Although all of the 3 gut microbiomes surveyed showed a high level of bacterial phyla *Firmicutes* and *Bacteroidetes*, analysis of the relative abundance of *Enterobacteriaceae* revealed a most significantly reduced population (Supplementary Figure 4).

To estimate the LPS biosynthetic genes of the samples, we annotated the predicted genes from the metagenomes using a LPS biosynthetic genes library derived from the KEGG orthologous groups. 0.0819 % (0d), 0.027 % (9w) and 0.0203 % (23w) of the sequences in the gut microbiome could be assigned to the LPS biosynthetic gene database, identified most genes involved in LPS biosynthetic pathway at 0d decreased markedly after intervention (Supplementary Figure 5 and 6) and the *Enterobacter* as the most changed genus in the

reconstructed metabolic map of his gut microbiota (Supplementary Figure 7).

Sequence-guided bacteria isolation. We used “sequence-guided isolation” to culture this *Enterobacter* population from the volunteer’s gut. About 200 colonies from the LB medium plates identified as possible *Enterobacter* sp. strains because their V3 sequences migrated to identical positions of the *Enterobacter* bands (Supplementary Figure 8). Finally, we obtained 106 pure strains which were classified into 5 DGGE and ERIC-PCR fingerprinting patterns and the representative isolates for each fingerprinting type were identified by 16S ribosomal RNA (rRNA) sequencing. One predominant isolate (B29) (DGGE fingerprint type D8), which was confirmed to be a member of the genus *Enterobacter* based on the 16S rRNA gene sequence, was picked and a spontaneous mutant for rifampicin resistance was selected for animal study.

Identification of the *Enterobacter cloacae* B29 strain. The bacterium was originally isolated from the human’s gut and was identified as *Enterobacter* sp., which belongs to the family *Enterobacteriaceae*. The identification of the isolate B29 was carried out by 16S rRNA gene sequencing after preliminary biochemical analysis. The 1.5 kb sequence of 16S rRNA gene showed 99 % similarity with *Enterobacter cloacae* (GenBank accession no. AB244457) and was also supported by biochemical identification performed with the VITEK 2 automated system using the ID-GN card (Supplementary Table1).

Endotoxin activity of the strain of *Enterobacter cloacae* B29 based on limulus

amebocyte lysate (LAL) test. Endotoxin activities of *Enterobacter cloacae* B29 and the positive control *E. coli* 055:B5 LPS measured by the LAL test were shown in Supplementary Figure 9. Sigma's lipopolysaccharides contain endotoxin levels of not less than 500,000 EU (endotoxin units)/mg unless otherwise noted; one nanogram of endotoxin is equivalent to 5 EU (Limulus lysate assay). The Endotoxin activities of *E. coli* 055:B5 lipopolysaccharide (Sigma) in our study was 3.67×10^6 EU mg⁻¹ LPS, agreed with the Sigma's instruction. LPS purified from the strain B29 had a high endotoxin activity up to 4.45×10^6 EU mg⁻¹ LPS, consistent with the endotoxin activity level of LPS from *E. coli* 055:B5 (Supplementary Figure 9).

Colonization of the gut of the germfree C57BL/6J mice by *Enterobacter cloacae* B29.

Inoculation of B29 once into germfree mice on normal chow diet (NCD) by gavage with as low as 100 cells led to a stable gut population of 10^{11} - 10^{12} cells/g feces one week after inoculation, consistent with the result under high inoculation dosage (10^{10} cells of B29/mouse) (Supplementary Figure 12), indicating that the bacterium can colonize the naive mouse gut and form a mono-associated gnotobiotic animal model. In animal study, we inoculated 10^{10} cells of B29 everyday for one week into mice under both normal chow (NCD) and high-fat diet (HFD) feeding conditions. B29 colonized mice gut to a high population level of 10^{10} - 10^{12} cells/g feces, which maintained for the following 15 weeks. The B29 strain reached a significantly higher population level in the gut of NCD-fed than HFD-fed animals (Supplementary Figure 13).

Supplementary references

- Caporaso, J. G., J. Kuczynski, et al. (2010). QIIME allows analysis of high-throughput community sequencing data. *Nature methods* **7**: 335-336.
- Di Cello, F., A. Bevivino, et al. (1997). Biodiversity of a Burkholderia cepacia population isolated from the maize rhizosphere at different plant growth stages. *Applied and environmental microbiology* **63**: 4485-4493.
- Dyszynski, G. and W. Sheldon (2006). RDPquery: A Java program from the Sapelo Program Microbial Observatory for automatic classification of bacterial 16S rRNA sequences based on Ribosomal Database Project taxonomy and Smith-Waterman alignment.
- Eckburg, P. B., E. M. Bik, et al. (2005). Diversity of the human intestinal microbial flora. *Science* **308**: 1635-1638.
- Edgar, R. C. (2010). Search and clustering orders of magnitude faster than BLAST. *Bioinformatics* **26**: 2460-2461.
- Hayashi, H., M. Sakamoto, et al. (2002). Phylogenetic analysis of the human gut microbiota using 16S rDNA clone libraries and strictly anaerobic culture-based methods. *Microbiology and immunology* **46**: 535.
- Hulton, C., C. Higgins, et al. (1991). ERIC sequences: a novel family of repetitive elements in the genomes of Escherichia coli, Salmonella typhimurium and other enterobacteria. *Molecular microbiology* **5**: 825-834.
- Ludwig, W., O. Strunk, et al. (2004). ARB: a software environment for sequence data. *Nucleic acids research* **32**: 1363-1371.
- Muyzer, G., E. C. De Waal, et al. (1993). Profiling of complex microbial populations by denaturing gradient gel electrophoresis analysis of polymerase chain reaction-amplified genes coding for 16S rRNA. *Applied and environmental microbiology* **59**: 695-700.
- Saulnier, D., G. R. Gibson, et al. (2008). In vitro effects of selected synbiotics on the human faecal microbiota composition. *FEMS microbiology ecology* **66**: 516-527.
- Schloss, P. D. and J. Handelsman (2005). Introducing DOTUR, a computer program for defining operational taxonomic units and estimating species richness. *Applied and environmental microbiology* **71**: 1501-1506.
- Thompson, J. R., L. A. Marcelino, et al. (2002). Heteroduplexes in mixed-template amplifications: formation, consequence and elimination by 'reconditioning PCR'. *Nucleic acids research* **30**: 2083-2088.
- Versalovic, J., T. Koeuth, et al. (1991). Distribution of repetitive DNA sequences in eubacteria and application to fingerprinting of bacterial genomes. *Nucleic acids research* **19**: 6823-6831.
- Zerbino, D. R. and E. Birney (2008). Velvet: algorithms for de novo short read assembly using de Bruijn graphs." *Genome research* **18**: 821-829.

Zhang, X., X. Yan, et al. (2005). Optimized sequence retrieval from single bands of temperature gradient gel electrophoresis profiles of the amplified 16S rDNA fragments from an activated sludge system. *Journal of microbiological methods* **60**: 1-11.

Supplementary Figures and Tables

Supplementary Table 1. Details of biochemical identification of the *Enterobacter cloacae* B29

strain using the Vitek 2 ID-GN system.

Well	Mnemonic	Test	Result ^a
2	APPA	Ala-Phe-Pro-ARYLAMIDASE	—
3	ADO	ADONITOL	+
4	PyrA	L-Pyrrolydonyl-ARYLAMIDASE	—
5	IARL	L-ARABITOL	—
7	dCEL	D-CELLOBIOSE	+
9	BGAL	BETA-GALACTOSIDASE	+
10	H2S	H2S PRODUCTION	—
11	BNAG	BETA-N-ACETYL-GLUCOSAMINIDASE	+
12	AGLTp	Glutamyl Arylamidase pNA	—
13	dGLU	D-GLUCOSE	+
14	GGT	GAMMA-GLUTAMYL-TRANSFERASE	—
15	OFF	FERMENTATION/ GLUCOSE	+
17	BGLU	BETA-GLUCOSIDASE	(—)
18	dMAL	D-MALTOSE	+
19	dMAN	D-MANNITOL	+
20	dMNE	D-MANNOSE	+
21	BXYL	BETA-XYLOSIDASE	+
22	BAlap	BETA-Alanine arylamidase pNA	—
23	ProA	L-Proline ARYLAMIDASE	+
26	LIP	LIPASE	—
27	PLE	PALATINOSE	+
29	TyrA	Tyrosine ARYLAMIDASE	+
31	URE	UREASE	—
32	dSOR	D-SORBITOL	+

33	SAC	SACCHAROSE/SUCROSE	+
34	dTAG	D-TAGATOSE	—
35	dTRE	D-TREHALOSE	+
36	CIT	CITRATE(SODIUM)	+
37	MNT	MALONATE	+
39	5KG	5-KETO-D-GLUCONATE	—
40	ILATk	L-LACTATE alkalinisation	+
41	AGLU	ALPHA-GLUCOSIDASE	(—)
42	SUCT	SUCCINATE alkalinisation	+
43	NAGA	Beta-N-ACETYL-GALACTOSAMINIDASE	+
44	AGAL	ALPHA-GALACTOSIDASE	+
45	PHOS	PHOSPHATASE	—
46	GlyA	Glycine ARYLAMIDASE	+
47	ODC	ORNITHINE DECARBOXYLASE	+
48	LDC	LYSINE DECARBOXYLASE	—
53	IHISa	L-HISTIDINE assimilation	—
56	CMT	COURMARATE	—
57	BGUR	BETA-GLUCORONIDASE	—
58	O129R	O/129 RESISTANCE (comp.vibrio.)	+
59	GGAA	Glu-Gly-Arg-ARYLAMIDASE	—
61	IMLTa	L-MALATE assimilation	—
62	ELLM	ELLMAN	—
64	ILATa	L-LACTATE assimilation	—

a, Calculations are performed on raw data and compared to thresholds to determine reactions for each test.

With the VITEK 2, test reaction results appear as “+”, “—”, “(—)” or “(+)”. Reactions that appear in parentheses are indicative of weak reactions that are too close to the test threshold.

Supplementary Table 2. Translocation of B29 into the inoculated mice on both high fat and normal chow feeding.

CFU g ⁻¹	Heart	Lung	Liver	Kidney	Spleen	Stomach	Small intestine	Cecum content
NCD+B29 (G2-7)	3300 ^a	15500	9800	530	19350	>10 ⁶	>10 ⁶	>10 ⁶
HFD+B29 (G4-2)	275	16000	937.5	495	9800	775	>10 ⁶	>10 ⁶

a, colony-forming units (CFU g⁻¹), counted after spread plating 100 µl supernatant onto LB agar

plates, which were cultured under 37°C condition for 16 hours; G2-7, mouse ID of NCD+B29 group (n=1);

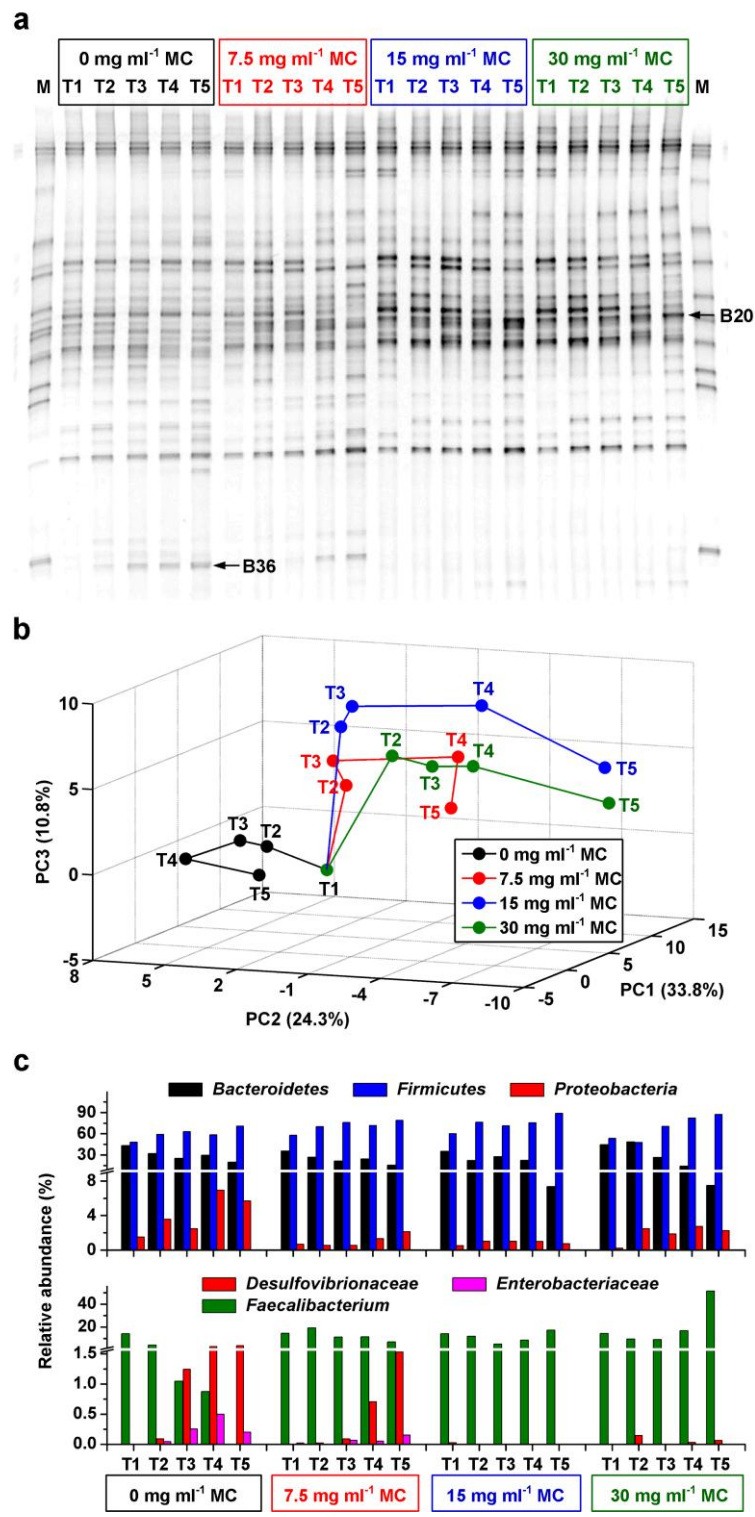
G4-2, mouse ID of HFD+B29 group (n=1).

Supplementary Table 3. Organ weights and small intestinal (SI) length of the *Enterobacter*-associated gnotobiotic model of obesity and its controls.

	Liver	Pancreas	Kidney	Spleen	Vastus	SI	Cecum weight	Cecum weight	Cecum
	weight (g)	weight (g)	weight (g)	weight (g)	lateralis	length	with contents	without contents	contents
					weight (g)	(cm)	(g)	(g)	(wet) (g)
NCD+LB	1.135 ^a	0.166	0.389	0.067 ^a	0.353 ^a	35.1	3.010 ^a	0.334 ^a	2.676 ^a
	(0.034)	(0.014)	(0.010)	(0.003)	(0.015)	(0.4)	(0.294)	(0.043)	(0.294)
NCD+B29	1.218 ^a	0.164	0.371	0.063 ^a	0.354 ^a	34.5	2.185 ^b	0.286 ^{ab}	1.899 ^{ab}
	(0.040)	(0.013)	(0.004)	(0.003)	(0.017)	(1.0)	(0.180)	(0.029)	(0.164)
HFD+LB	1.135 ^a	0.168	0.388	0.070 ^a	0.387 ^a	33.8	1.968 ^b	0.250 ^{ab}	1.718 ^b
	(0.028)	(0.012)	(0.014)	(0.005)	(0.008)	(0.7)	(0.104)	(0.027)	(0.094)
HFD+B29	1.585 ^b	0.207	0.413	0.089 ^b	0.446 ^b	31.6	0.865 ^c	0.201 ^b	0.664 ^c
	(0.138)	(0.022)	(0.010)	(0.005)	(0.011)	(1.2)	(0.049)	(0.027)	(0.042)

Data were shown as means (S.E.M). Values of each group with same letters are not significantly different ($p > 0.05$) ($n=6$).

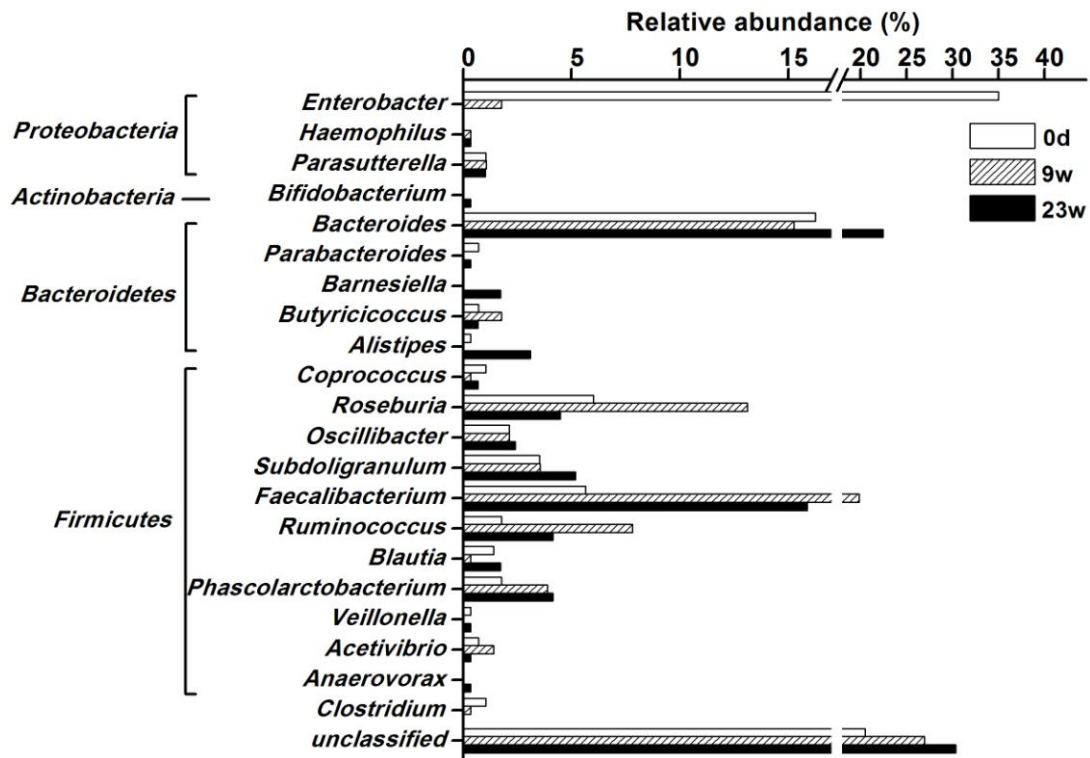
Supplementary Figure 1



Supplementary Figure 1. Bitter melon markedly modulated the human gut microbiota in *in vitro* experiment. (a) PCR-DGGE fingerprinting of the V3 region of 16S rRNA genes. (b) PCA score plot of the digitalized data of DGGE fingerprinting. Each circle represents the distance between a particular sample

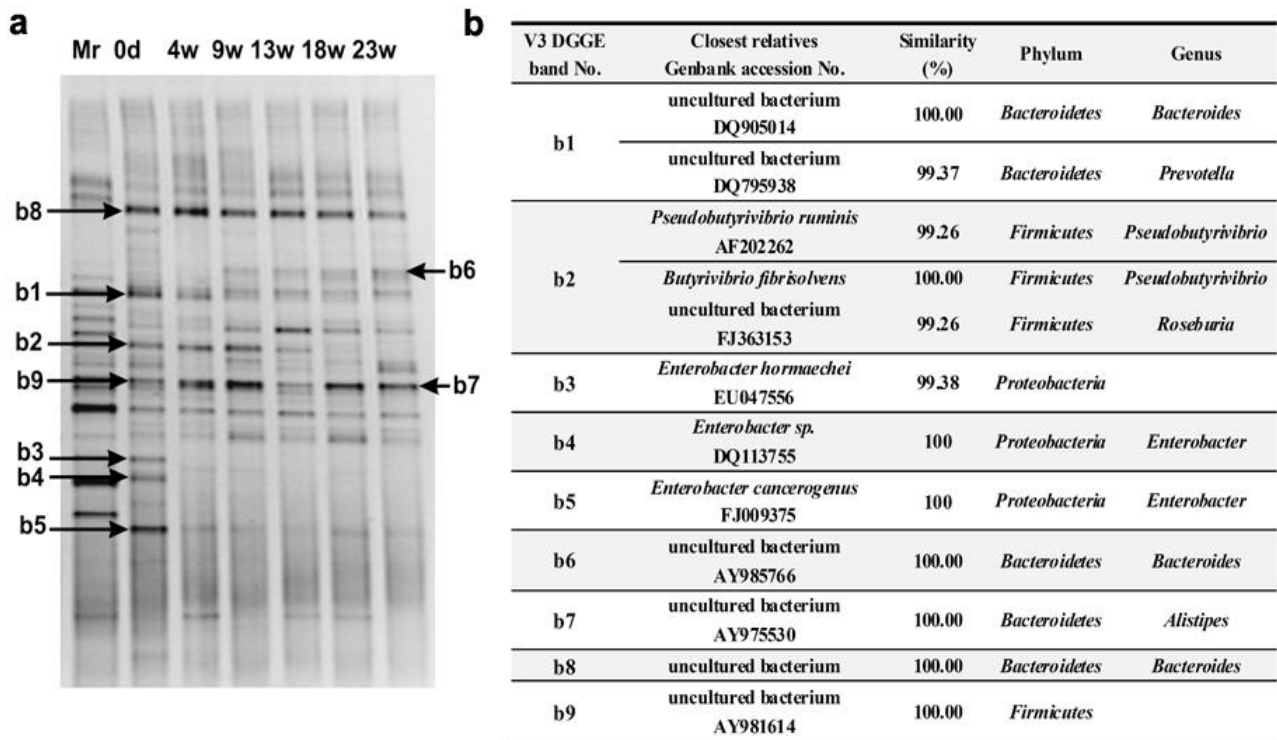
and its control sample at 0 hour. (c) Taxon-based analysis of the microbial community structure in response to the treatment of bitter melon as determined by bar-coded 454 pyrosequencing. Bacteria numbers are expressed as the proportion of total intestinal microbiota. MC stands for bitter melon; T1, T2, T3, T4, and T5 stand for the 0, 6, 12, 24, and 48 hours of incubation time, respectively.

Supplementary Figure 2



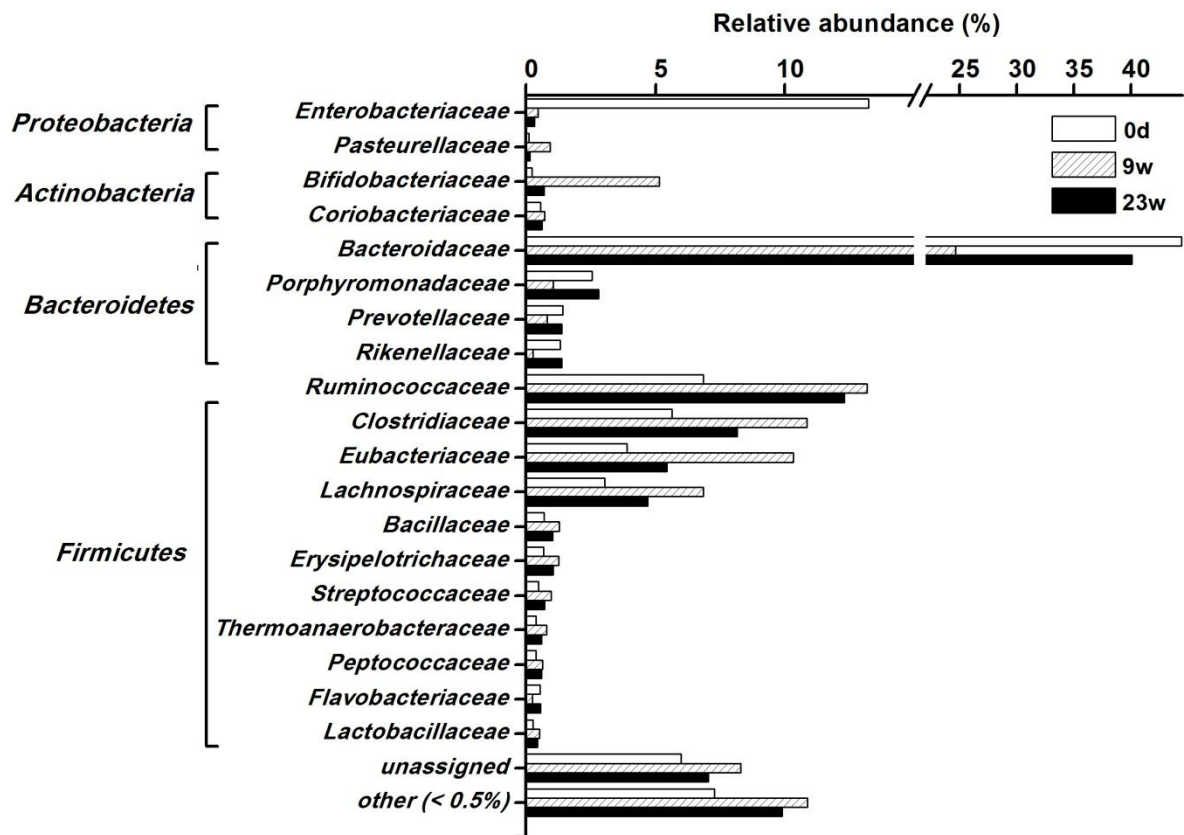
Supplementary Figure 2. Abundance shifts of *Enterobacter* revealed by clone library analysis of the near full-length 16S rRNA gene in the morbidly obese volunteer during weight loss.

Supplementary Figure 3



Supplementary Figure 3. Structural changes of gut microbiota and identification of *Enterobacter* in the DGGE fingerprint based on the V3 region of the 16S rRNA gene in the morbidly obese volunteer during weight loss. a. DGGE gel for the predominant bacteria (V3 region of 16S rRNA gene diversity profiling); the bands with arrows were selected predominant ones. b. sequenced bands from the V3 DGGE gel.

Supplementary Figure 4

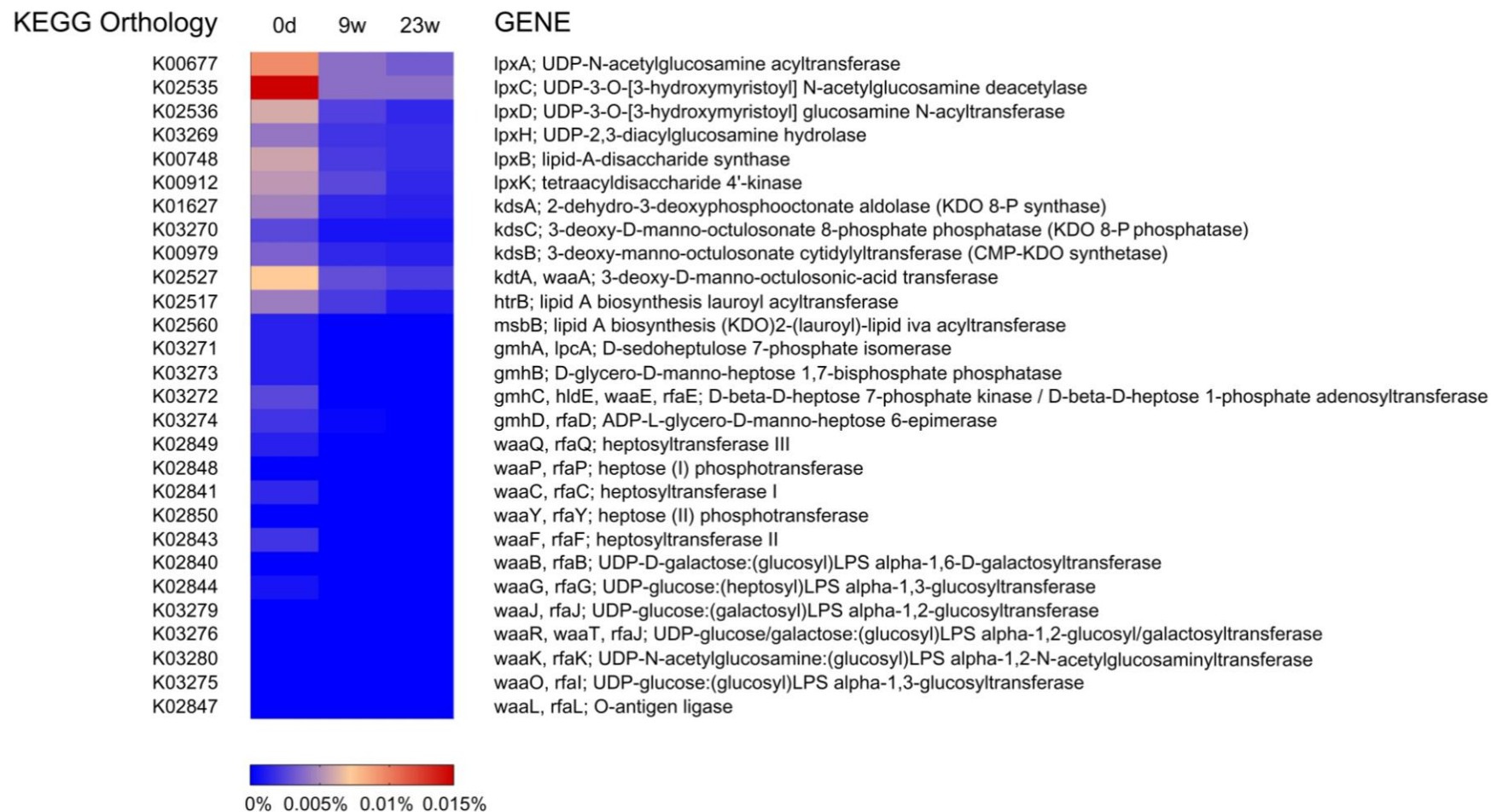


Supplementary Figure 4. Abundance shifts of *Enterobacteriaceae* revealed by metagenomic sequencing in the morbidly obese volunteer during weight loss. The relative abundance of each family member in the gut microbiota was calculated using taxon-based analysis of the microbial community structure based on the metagenomic sequencing of the fecal samples at 0d, 9w and 23w. Others (< 0.5%), families which relative abundance were less than 0.5%.

Supplementary Figure 5. Changes in the LPS biosynthetic pathway revealed by metabolic reconstruction based on metagenomic sequences in the morbidly obese volunteer during weight loss. Red color, KOs which decreased their relative abundances after 23-week intervention, and the changes in the abundance of these LPS biosynthetic genes in the morbidly obese volunteer during weight loss were shown in Fig. S6.

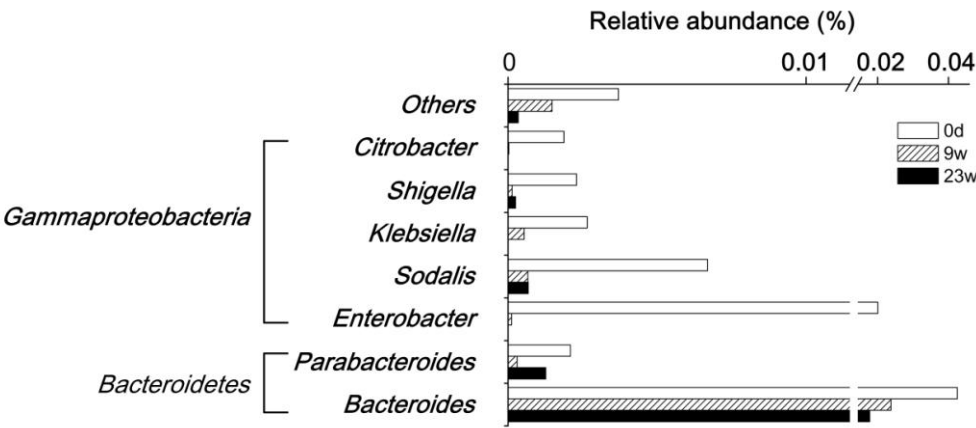
[illegible]

Supplementary Figure 6



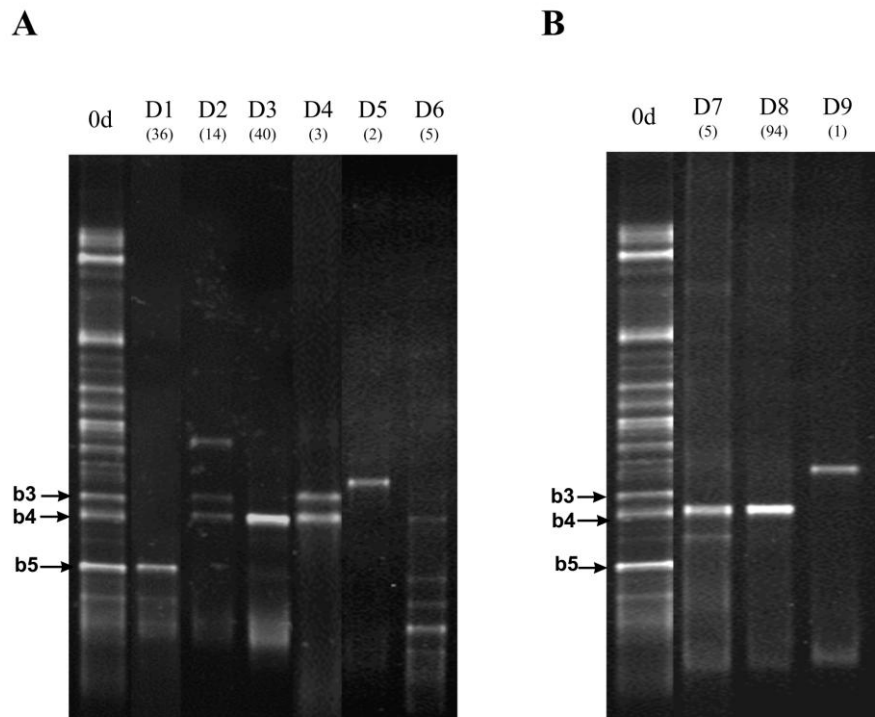
Supplementary Figure 6. Changes in the abundance of LPS biosynthetic genes in the morbidly obese volunteer during weight loss.

Supplementary Figure 7



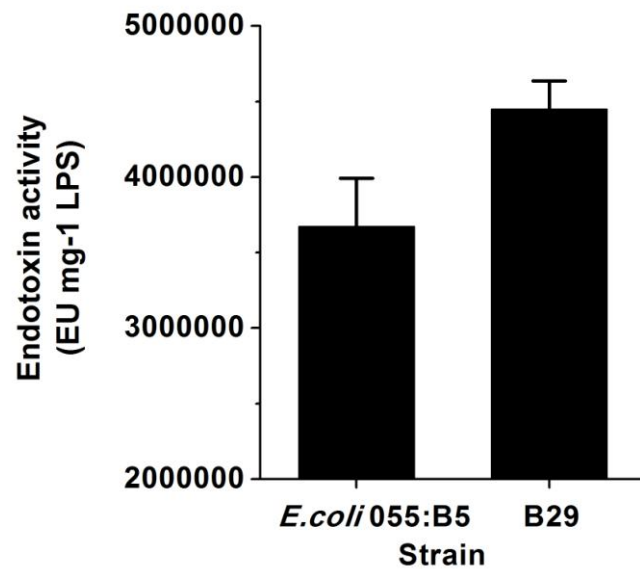
Supplementary Figure 7. Abundance shifts of LPS biosynthetic genes at the genus level, revealed by metagenomic sequencing in the morbidly obese volunteer during weight loss.

Supplementary Figure 8



Supplementary Figure 8. Screening of candidate *Enterobacter* isolates based on their co-migration pattern with the *Enterobacter* bands in the DGGE fingerprint of baseline sample of the morbidly obese volunteer. A, B, two colony morphologies; Lane 1 of A, B, the structure of gut microbiota based on the V3 region of the 16S rRNA gene in the morbidly obese volunteer at 0 day. Lane D1 to D9, types of DGGE fingerprint of different isolates. Numbers in brackets mean the number of isolates of every DGGE fingerprint type. b3, b4 and b5, the three predominant bands in the volunteer's baseline DNA fingerprint which were found to contain V3 sequences of the 16S rRNA gene of *Enterobacter* (Supplementary Figure 3).

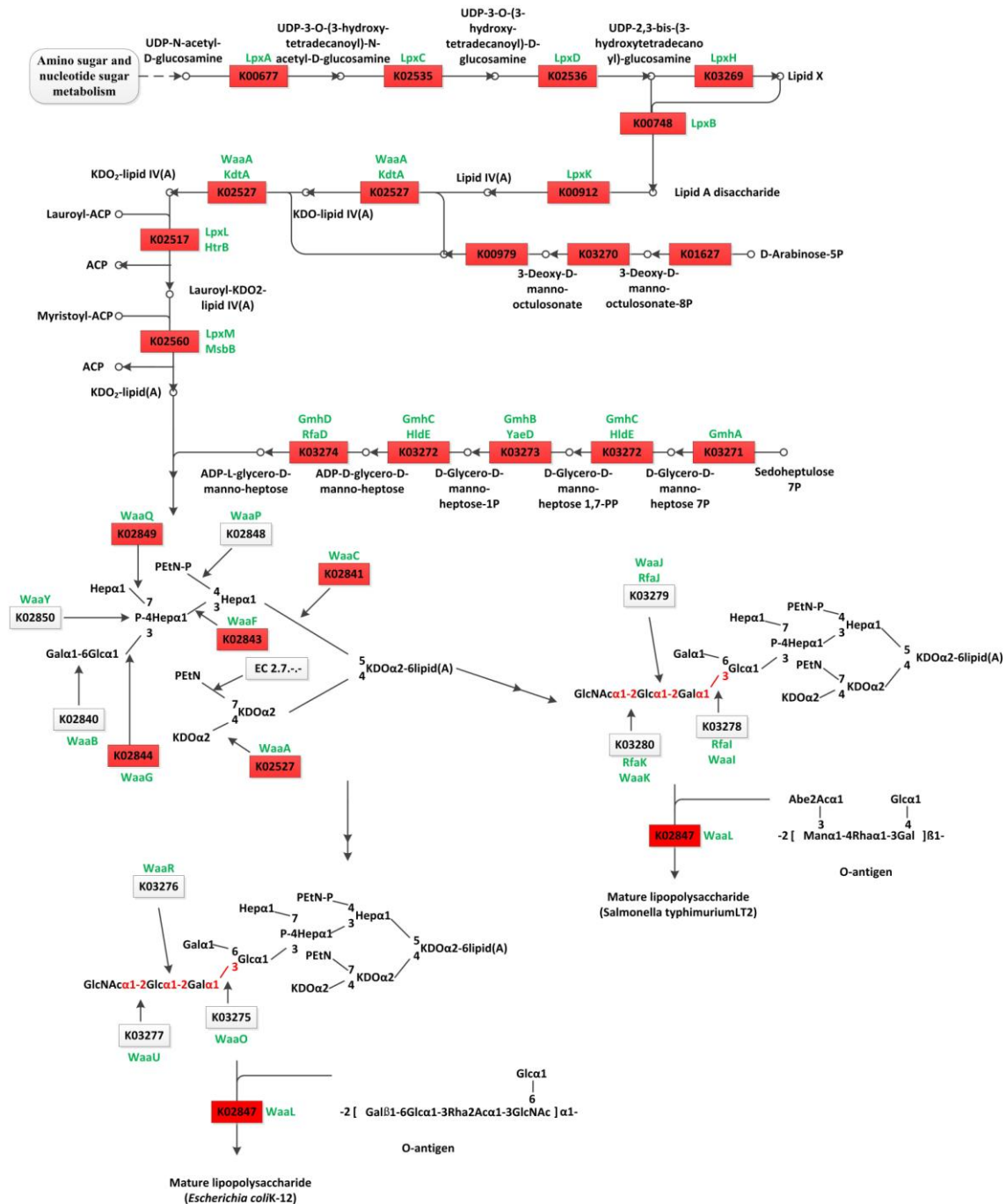
Supplementary Figure 9



Supplementary Figure 9. Endotoxin activity of the strain of *Enterobacter cloacae* B29 based on limulus amebocyte lysate (LAL) test. *E. coli* 055:B5, *E. coli* 055:B5 LPS (Sigma) was used as a positive control.

Supplementary Figure 10

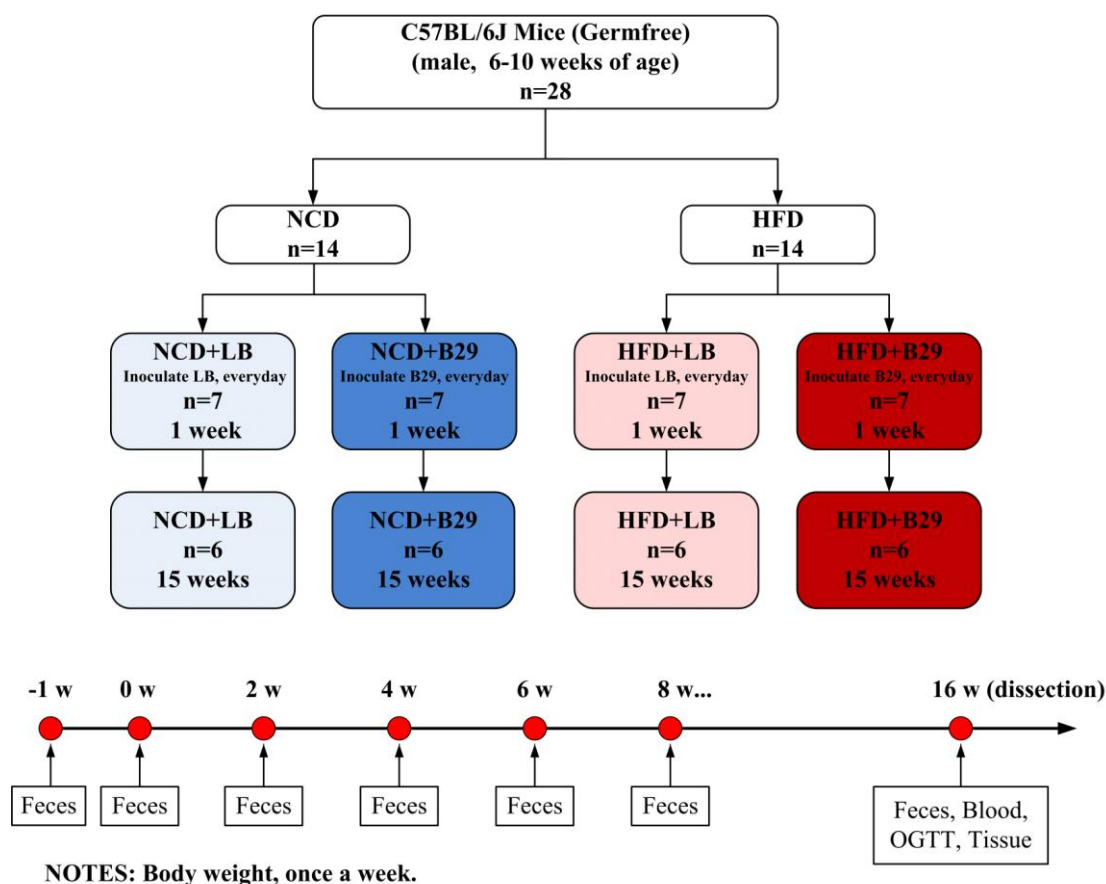
LIPOPOLYSACCHARIDE BIOSYNTHESIS



Supplementary Figure 10. LPS biosynthetic pathway based on genome sequence of B29. Red color,

KOs which annotated in genome sequence of *Enterobacter cloacae* B29

Supplementary Figure 11



Supplementary Figure 11. Experimental design for establishment of the *Enterobacter*-associated

gnotobiotic model of obesity. NCD, normal chow diet; HFD, high fat diet; LB: Luria-Bertani medium;

B29, bacteria strain B29, oral inoculating dose: 10^{10} cells of B29/mouse in 0.1ml of sterile PBS.

NCD+LB group: inoculated by gavage with 0.1ml sterile LB medium everyday for one week fed on

normal chow diet; NCD+B29 group: inoculated by gavage with 10^{10} cells of B29/mouse in 0.1ml sterile

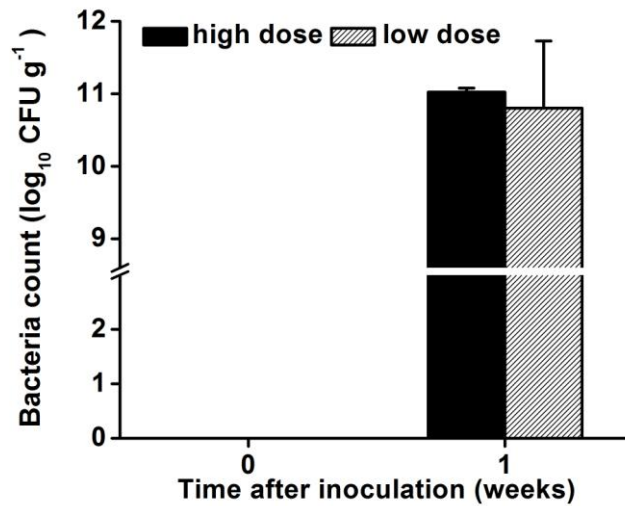
LB medium everyday for one week under normal chow diet; HFD+LB group: inoculated by gavage with

0.1ml sterile LB medium everyday for one week fed with high-fat diet; HFD+B29 group: inoculated by

gavage with 10^{10} cells of B29/mouse in 0.1ml sterile LB medium everyday for one week fed on high-fat

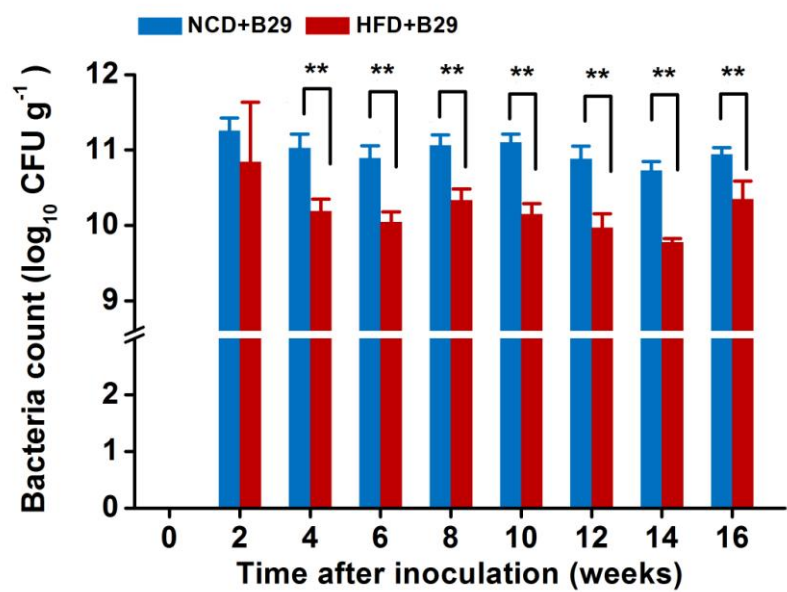
diet.

Supplementary Figure 12



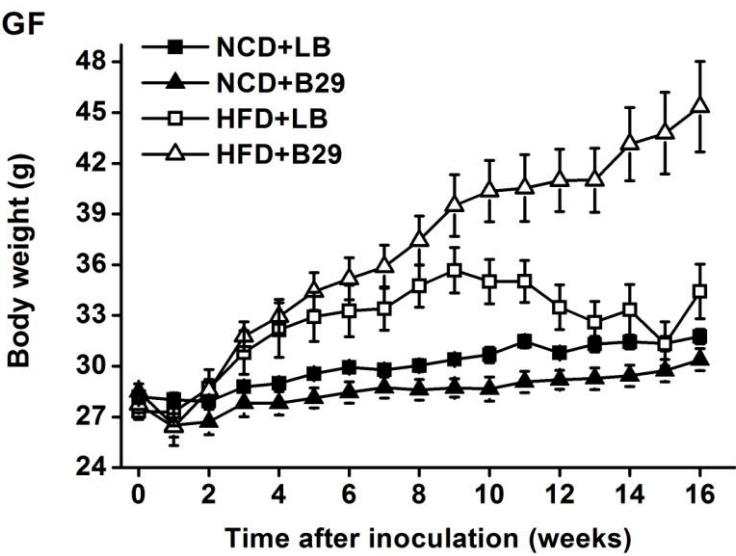
Supplementary Figure 12. Colonization of the gut of the germfree C57BL/6J mice by *Enterobacter cloacae* B29 under different inoculation dosages. Bacteria in the feces of inoculated mice were enumerated by plating for CFU (n = 6). Data were shown as means \pm S.E.M. High dose, 10^{10} cells of B29/mouse; low dose, 100 cells of B29/mouse.

Supplementary Figure 13



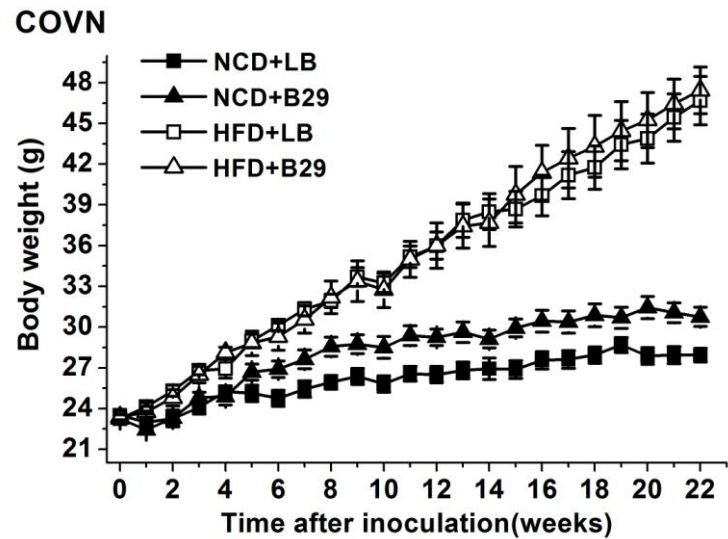
Supplementary Figure 13. opulation levels of *Enterobacter cloacae* B29 in the *Enterobacter*-associated gnotobiotic model of obesity and controls. Data were shown as means \pm S.E.M. (n=6). ** $P < 0.01$.

Supplementary Figure 14



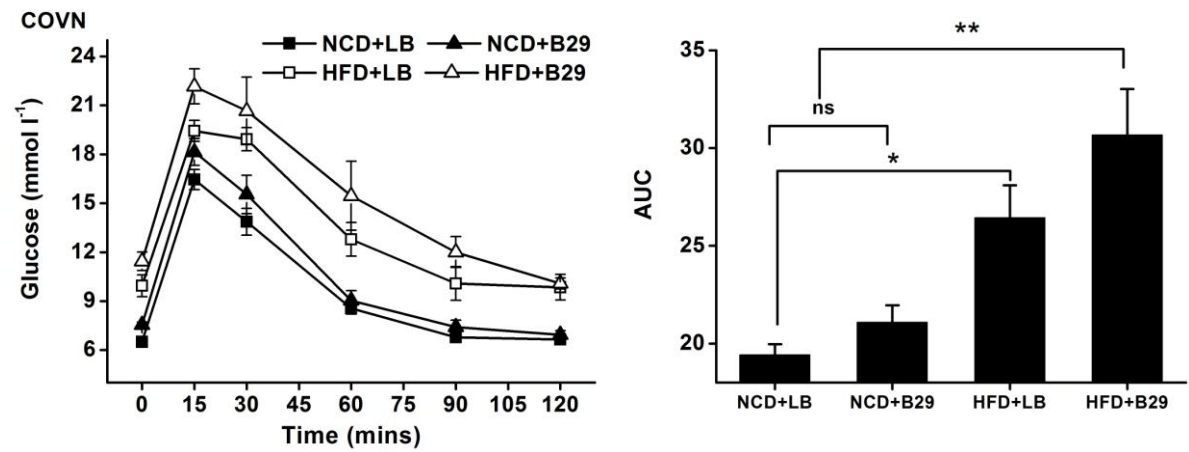
Supplementary Figure 14. Growth curve of *Enterobacter cloacae* B29-associated germfree obese mice and controls. Data were shown as means \pm S.E.M (n=6). GF, germfree.

Supplementary Figure 15



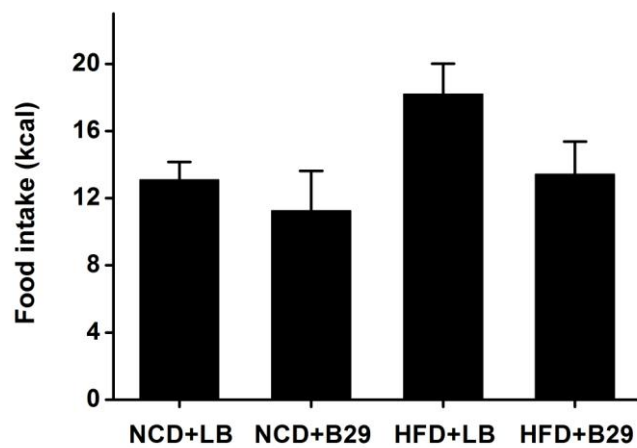
Supplementary Figure 15. Growth curve of high fat diet-induced conventional mice. Data were shown as means \pm S.E.M (n=8). COVN, conventional mice.

Supplementary Figure 16



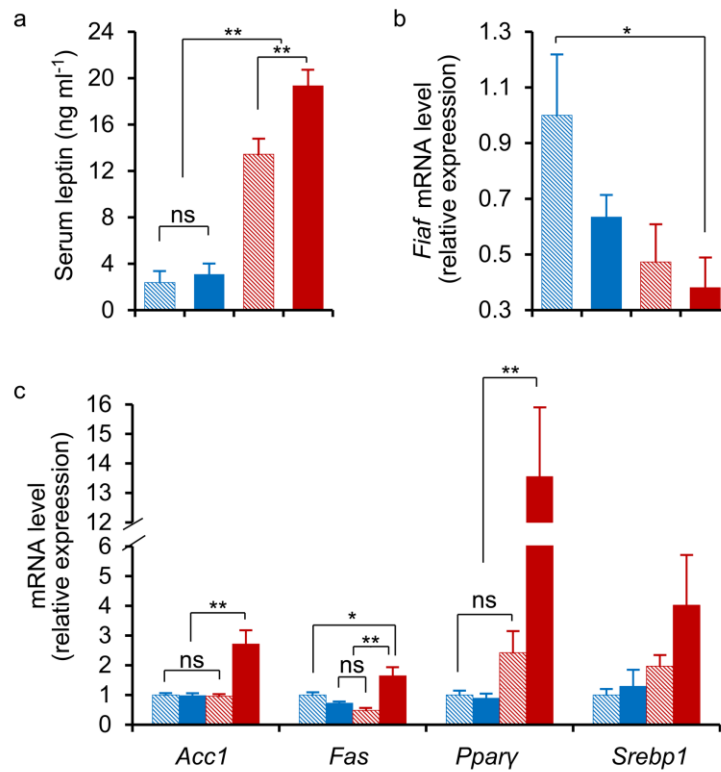
Supplementary Figure 16. Oral glucose tolerance test (OGTT) of high fat diet-induced conventional mice. Data were shown as means \pm S.E.M (n=8). COVN, conventional mice.

Supplementary Figure 17



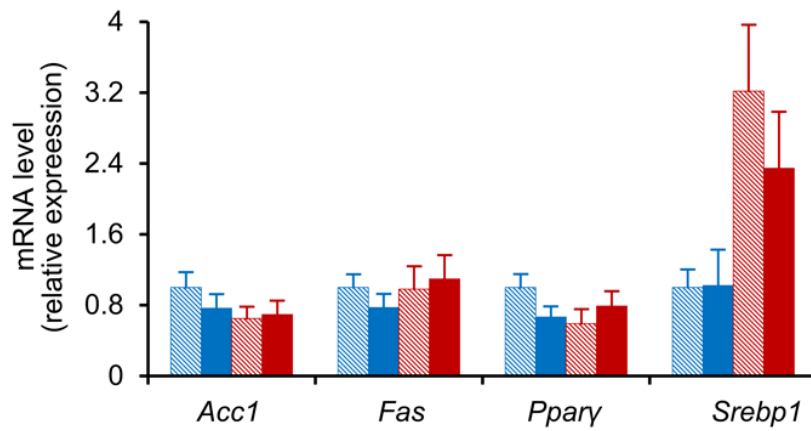
Supplementary Figure 17. 24h-food intake of *Enterobacter cloacae* B29-associated germfree obese mice and controls. Data were shown as means \pm S.E.M (n=3).

Supplementary Figure 18



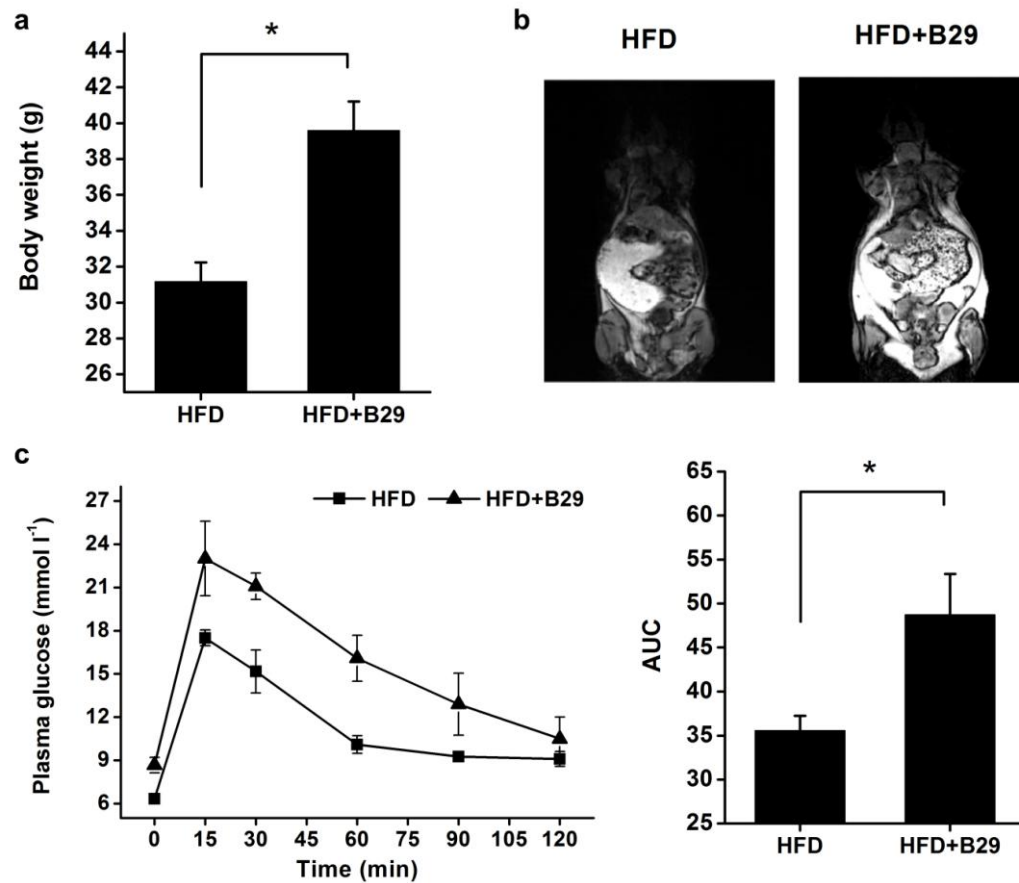
Supplementary Figure 18. Distorted lipid metabolism in the *Enterobacter*-induced obese mice (Data collected at the end of 16 weeks after inoculation). ELISA analysis of serum leptin (a); RT- quantitative PCR analysis of expression of *Fiaf* in the ileum (b), of *Acc1*, *Fas* and *Pparγ* in the liver (c). All mRNA quantification data were normalized to the housekeeping gene Glyceraldehyde-3-phosphate dehydrogenase (*Gapdh*). Gene expression levels were expressed as values relative to the control group (NCD+LB) (n=6). ns, no significant difference; * $P < 0.05$; ** $P < 0.01$. Color code for animal groups: NCD+LB: blue slash; NCD+B29: blue; HFD+LB: red slash; HFD+B29: red.

Supplementary Figure 19



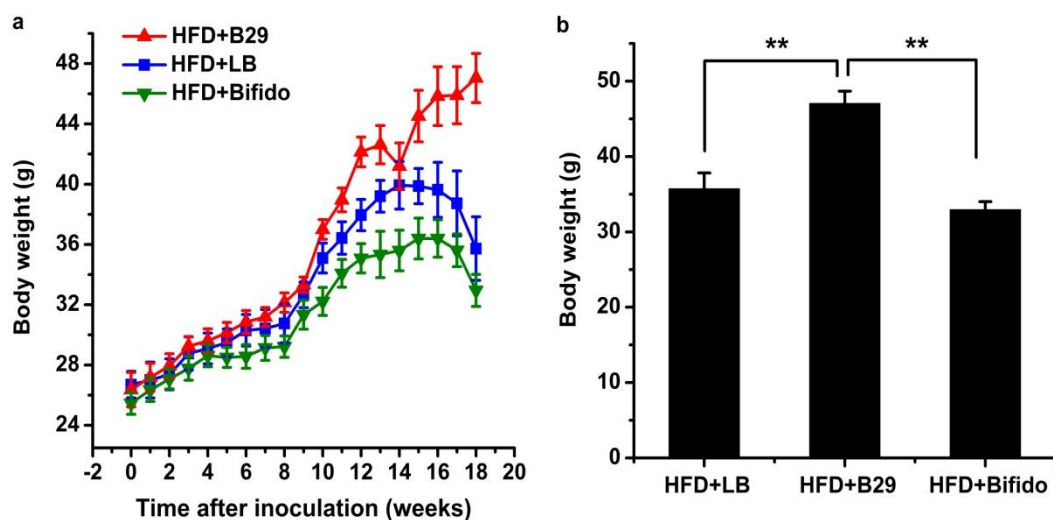
Supplementary Figure 19. Reverse transcription (RT)-quantitative PCR analysis of expression of *Acc1*, *Fas* and *Ppar* in the epididymal fat pad. All mRNA quantification data were normalized to the housekeeping gene Glyceraldehyde-3-phosphate dehydrogenase (*Gapdh*). Gene expression levels were expressed as values relative to the control group (NCD+LB) (n = 6). Color code for animal groups: NCD+LB: blue slash; NCD+B29: blue; HFD+LB: red slash; HFD+B29: red.

Supplementary Figure 20



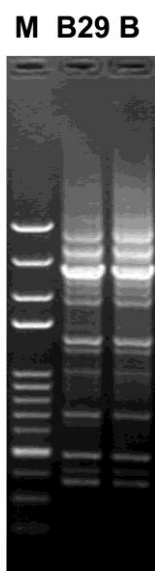
Supplementary Figure 20. Repeated animal trial confirmed that *Enterobacter cloacae* B29 caused obesity and insulin resistance in germfree mice under HFD-feeding for 12 weeks. a. Body weight at the end of the trial; b. MRI image showing fat distribution; c. Glucose tolerance test at the end of the trial. Mice were intraperitoneally injected with glucose (2 g/kg body weight). Data were shown as means \pm S.E.M. P values were determined using the t-test (n=3 of HFD and 5 of HFD +B29). * $P < 0.05$. HFD, control group, mice fed with high-fat diet for 12 weeks; HFD +B29, mice inoculated with B29 and fed with high-fat diet for 12 weeks.

Supplementary Figure 21



Supplementary Figure 21. Growth curve and body weight of *Enterobacter cloacae* B29- and *Bifidobacterium animalis*-associated germfree mice and controls via alternation of normal chow diet and high fat diet. a. Growth curve; b. Body weight by the end of the trial. In the first 8 weeks, 6- to 10-week-old germfree mice (n=4~6 per group) mice were fed normal chow diet; in the following 10 weeks, the mice were changed to high-fat diet. HFD, high-fat diet; LB, Luria-Bertani medium; B29, bacteria strain B29, oral inoculating dose: 10^{10} cells of B29/mouse in 0.1ml of sterile PBS; Bifido, *Bifidobacterium animalis*, oral inoculating dose, 10^{10} cells of Bifido/mouse in 0.1ml of sterile PBS. HFD+LB group, inoculated by gavage with 0.1ml sterile LB medium once; HFD+B29 group, inoculated by gavage with 10^{10} cells of B29/mouse in 0.1ml sterile LB medium once; HFD+Bifido group, inoculated by gavage with 10^{10} cells of Bifido/mouse in 0.1ml sterile LB medium once. Normally distributed and independent data are shown as means \pm S.E.M. P values were determined using the one-way ANOVA test followed by Tukey's test. **, $P < 0.01$.

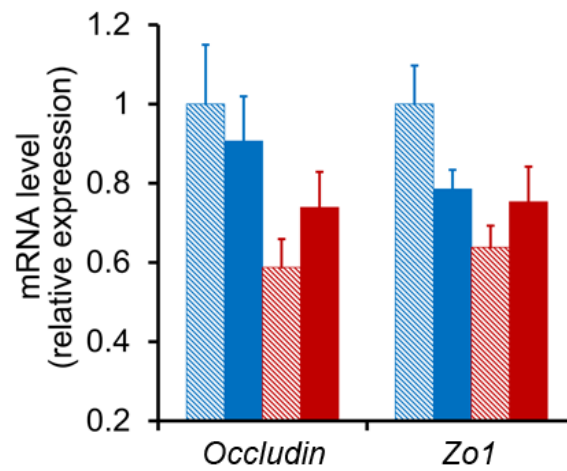
Supplementary Figure 22



Supplementary Figure 22. Re-isolation and identification of *Enterobacter cloacae* B29 from the *Enterobacter*-associated gnotobiotic model of obesity based on ERIC-PCR genomic fingerprinting.

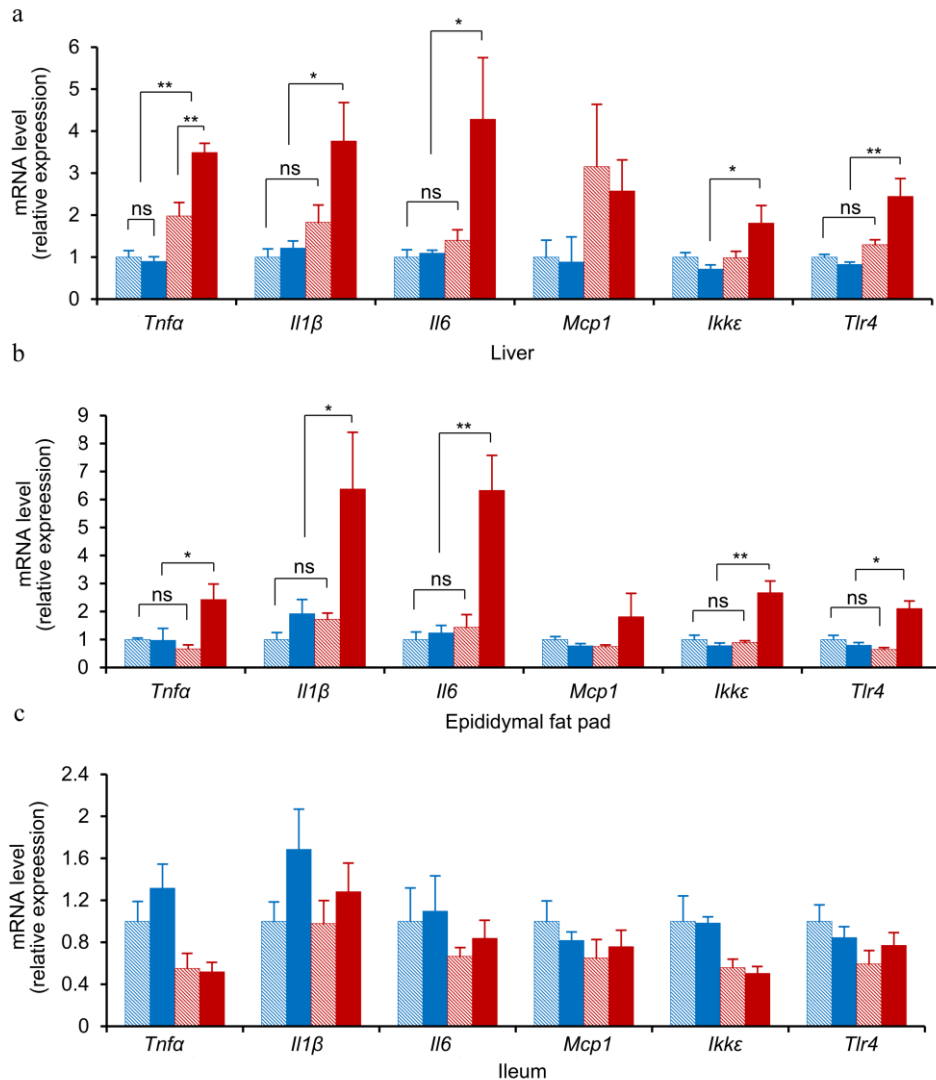
Lane M, DNA size marker (100-bp ladder); B, re-isolated strain from feces of the gnotobiotic mice.

Supplementary Figure 23



Supplementary Figure 23. Reverse transcription (RT)-quantitative PCR analysis of the gene expression of the two tight junction proteins occludin and ZO-1 in the ileum. All mRNA quantification data were normalized to the housekeeping gene Glyceraldehyde-3-phosphate dehydrogenase (GAPDH). Gene expression levels were expressed as values relative to the control group (NCD+LB) (n =6). Color code for animal groups: NCD+LB: blue slash; NCD+B29: blue; HFD+LB: red slash; HFD+B29: red.

Supplementary Figure 24



Supplementary Figure 24. Provoked local inflammation in the *Enterobacter*-induced obese mice

(Data collected at the end of 16 weeks after inoculation). Reverse transcription (RT)-quantitative PCR

analysis of expression of *Tnfa*, *Il1*, *Il6*, *Mcp1*, *Ikke* and *Tlr4* in the liver (a), epididymal fat pad (b) and

ileum (c). All mRNA quantification data were normalized to the housekeeping gene

Glyceraldehyde-3-phosphate dehydrogenase (*Gapdh*). Gene expression levels were expressed as values

relative to the control group (NCD+LB) (n=6). ns, no significant difference; * $P < 0.05$; ** $P < 0.01$. Color

code for animal groups: NCD+LB: blue slash; NCD+B29: blue; HFD+LB: red slash; HFD+B29: red. *Tnfa*, tumor necrosis factor-alpha gene; *Il1*, interleukin-1 gene; *Il6*, interleukin-6 gene; *Mcp1*, monocyte chemoattractant protein-1 gene; *Ikkε*, I kappa B kinase epsilon gene; *Tlr4*, toll-like receptor 4 gene.